INFO 0591-1

REPORT

RAPPORT

Atomic Energy Control Board
Commission de contrôle de l'énergie atomique

Canada

INFO-0591-1

REPORT

An Experimental Investigation of Fission Product Release in SLOWPOKE-2 Reactors

by

A.M.C. Harnden
B.J. Lewis and L.G.I. Bennett

Prepared for
the Atomic Energy Control Board
under its Regulatory Research
and Support Program
Ottawa, Canada

AECB Project No. 2.197.1

September 1995

Atomic Energy Control Board | Commission de contrôle de l'énergie atomique

Canada

AN EXPERIMENTAL INVESTIGATION OF FISSION PRODUCT RELEASE IN SLOWPOKE-2 REACTORS

A report prepared by A.M.C. Harnden, Department of Physics, Queen's University, and B.J. Lewis and L.G.I. Bennett, SLOWPOKE-2 Facility and the Department of Chemistry and Chemical Engineering, Royal Military College of Canada, under contract to the Atomic Energy Control Board.

ABSTRACT

Increasing radiation fields due to a release of fission products in the reactor container of several SLOWPOKE-2 reactors fuelled with a highly-enriched uranium (HEU) alloy core have been observed. It is believed that these increases are associated with the fuel fabrication where a small amount of uranium-bearing material is exposed to the coolant at the end-welds of the fuel element.

To investigate this phenomenon samples of reactor water and gas from the headspace above the water have been obtained and examined by gamma spectroscopy methods for reactors of various burnups at the University of Toronto, Ecole Polytechnique and Kanata Isotope Production Facility. An underwater visual examination of the fuel core at Ecole Polytechnique has also provided information on the condition of the core. This report (Volume 1) summarizes the equipment, analysis techniques and results of tests conducted at the various reactor sites. The data report is published as Volume 2.

RÉSUMÉ

On a observé une augmentation des champs de rayonnement causés par un rejet de produits de fission dans l'enceinte de plusieurs réacteurs SLOWPOKE-2 alimentés par un cœur en alliage d'uranium hautement enrichi (UHE). On croit qu'il y a un lien entre cette augmentation et la fabrication du combustible au cours de laquelle une faible quantité de matière uranifère est exposée au caloporteur au niveau des soudures terminales de l'élément de combustible.

Afin d'étudier ce phénomène, on a obtenu des échantillons d'eau de réacteur et de gaz provenant de la chambre d'expansion au-dessus de l'eau, qu'on a examinés par spectroscopie gamma appliquée à des réacteurs à taux de combustion divers à l'Université de Toronto, à l'École polytechnique et à l'Établissement de production d'isotopes de Kanata. Un examen visuel du cœur du combustible effectué sous l'eau à l'École polytechnique a fourni aussi des renseignements sur l'état du cœur. Ce rapport (volume 1) présente un résumé du

matériel utilisé, des techniques d'analyse et des résultats de tests effectués aux divers sites de réacteurs. Le rapport de données est publié sous le volume 2.

AN EXPERIMENTAL INVESTIGATION OF FISSION PRODUCT RELEASE IN SLOWPOKE-2 REACTORS

TABLE OF CONTENTS

LIST OF ACRONYMS AND SYMBOLS

ADC	Analog to Digital Converter
EP	Ecole Polytechnique
HEU	Highly Enriched Uranium
KIPF	Kanata Isotope Production Facility
LEU	Low Enriched Uranium
MCA	Multi Channel Analyzer
RMC	Royal Military College
S-G	Savitzky-Golay
U of T	University of Toronto
a	Diffusion parameter (fissions $s^{-1/2}$)
c	Recoil component of release (fissions/s)
C_g	Isotopic activity concentration in reactor gas headspace (Bq/L)
C(L)	Isotopic activity concentration at the top of the water column (Bq/L)
C_{meas}	Isotopic activity concentration measured in the water samples (Bq/L)
C_o	Isotopic activity concentration in the water at the reactor core (Bq/L)
C_{wo}	Initial isotopic activity concentration in reactor water (Bq/L)
C_w , $<C>_{av}$	Average isotopic activity concentration in reactor water (Bq/L)
D_f'	Empirical diffusion coefficient (s^{-1})
F	Fission rate per pin (fissions/s/pin)
F_c	Average core fission rate (fissions/s)
ℓ	Length of fuel pin (m)
L	Height of the water column (m)
n	Number of defective fuel pins per core
N_g	Number of atoms in reactor gas headspace
N_w	Number of atoms in reactor container water
r	Radius of fuel pin (m)
R_{fw}	Release rate from fuel to reactor water (atoms/s)
R_{wg}	Release rate from reactor water to gas headspace (atoms/s)
S	Fuel surface area per pin (m^2)
ΔS	Exposed fuel surface area per pin (m^2)
$T = (L/v)$	Transport time from reactor core to intake pipe (s)
t'	Transport time from intake pipe to sampling station (s)
$t_{tr} = T + t'$	Total transport time from core to sampling station (s)
v	Convective flow velocity (m/s)
V	Fuel volume per pin (m^3)
V_g	Volume of gas headspace (108 L)
V_w	Volume of reactor container water (1380 L)
Y	Fission yield (atoms/fission)
μ	Average fission fragment range in fuel (m)
λ	Decay constant (= ln(2)/half-life) (s^{-1})

AN EXPERIMENTAL INVESTIGATION OF FISSION PRODUCT RELEASE IN SLOWPOKE-2 REACTORS

1. INTRODUCTION

Following fabrication of the highly enriched uranium (HEU) fuel elements for the SLOWPOKE-2 research reactor, an external uranium contamination of the weld area was observed. This contamination occurred during the welding of end caps to the fuel pin meat, where some of the uranium aluminum alloy fuel was locally heated above its melting temperature and flowed out of the weld location. Although the weld area was machined later to remove such material, external contamination still remained (see Figure 1).[1]

In subsequent operation of several HEU-fuelled SLOWPOKE-2 reactors, radionuclides have been observed in the reactor container water that surrounds the fuel, but not in the pool water which, in turn, surrounds the reactor container. The gamma radiation fields around the reactor can generally be attributed to this build-up of radionuclides, although no radiological hazard has resulted. At present, the radiation fields at the higher burnup SLOWPOKE-2 facilities such as Ecole Polytechnique and the University of Toronto reach levels sufficient to activate the medium-level radiation alarms positioned above the reactor container after only a few hours of reactor operation at high power. Although these alarms were initially installed to detect the loss of pool water shielding or maloperation of the control rod, they are now being triggered in the day-to-day normal operation of the reactors at which point the reactors must be shut down. While it is believed that the observed increases in radiation dose rates are associated with the above mentioned complication in fuel fabrication, it is necessary to establish whether there are any other contributing causes.

By measuring the fission product release rate from the fuel to the reactor container water, it is possible to distinguish between release mechanisms and therefore to determine whether the increase in radiation fields around the reactor is due to external contamination of the fuel elements or due to a loss of integrity of the fuel sheath. This information can also be used to estimate the levels of activity to be anticipated in future operation of the lower-burnup cores.

This report summarizes the experimental techniques, method of analysis, and results of studies conducted at the SLOWPOKE-2 facilities of the Royal Military College (RMC), the University of Toronto (U of T), Ecole Polytechnique (EP), and the Kanata Isotope Production Facility (KIPF). Although the reactor at RMC is the only SLOWPOKE-2 to be fuelled with a low-enriched uranium (LEU) core of uranium dioxide, it has provided a convenient location to commission the experimental equipment for fission product analysis. A visual examination of the uranium alloy core at EP with an underwater television camera has also been performed to compliment the fission product release study and to provide information on the condition of the core.

2. SLOWPOKE-2 REACTOR DESIGN

The name SLOWPOKE is an acronym for Safe LOW POwer (K) critical Experiment, a research reactor developed by Atomic Energy of Canada Limited. This reactor is inherently safe since increasing temperatures would produce a negative effect on excess reactivity.[1] The reactor produces a flux of 1.0×10^{12} neutrons/cm^2/s and 20 kW of thermal energy at full power. Seven of these reactors are now operating across Canada and one is located at the University of the West Indies, in Kingston, Jamaica.

The SLOWPOKE-2 reactor is a tank-in-pool type of design with a light-water moderated core within a reactor container structure (see Figure 2).[2] The surrounding pool of light-water serves as radiation shielding for research personnel and also as a secondary heat sink. Water purity is maintained by circulating the container water through a series of deionizer columns on a weekly basis. Control of the reactor is maintained with a single control rod. The radiation monitors are located just above the reactor container (the medium-level alarm), above the reactor on the ceiling of the room (the area alarm), and beside the deionizer columns (low-level alarm). Generally, only the medium-level alarm prohibits continuous full-power operation.

2.1 Fuel Design

Of the eight operating SLOWPOKE-2 reactors, seven were fuelled with 93% U-235 enriched uranium aluminum alloy fuel pins coextruded with ASTM 1050-Aluminum cladding. The most recently commissioned SLOWPOKE-2 reactor (which is operating at RMC) is fuelled with low enriched uranium oxide fuel (20% U-235), clad in Zircaloy-4. A comparison of the two types of cores is given in Table 1. Radiation fields associated with fission product release from these cores have been observed only at those reactors fuelled with the HEU fuel.

3. EXPERIMENTAL DETAILS

3.1 Equipment

An analysis of fission products in the reactor container water and gas headspace at four SLOWPOKE-2 reactors has been performed by gamma ray spectroscopy methods. A GMX high purity germanium detector with a thin beryllium window (EG&G Ortec) was used to detect photons with energies between 80 and 2500 keV. For ease of portability, the detector bias supply (-3000 V), signal amplifier, and analog to digital converter (ADC) are integrated into one self-contained instrument, the Canberra model 1510. From the ADC, the signals are passed to a Canberra S100 (386) multi-channel analyzer (MCA) which is resident on a printed circuit board inside an IBM PS/2 P70 portable computer. Control over the MCA is obtained via a Windows 3.0 driven software package supplied by Canberra-Packard. The

pile-up rejection feature of the ADC was not used since the dead time of the water and gas samples was low.

Radiation shielding of the detector was provided by a transportable ensemble consisting of a lead brick castle supported by a sturdy aluminum frame (see Figure 3). Both the lead bricks and the structure may be disassembled in less than one-half hour and placed in their respective shipping containers for transit in a panel van. Background levels over the 2500 keV range were reduced to 180 counts per minute by the 10-cm thick lead bricks and a series of cadmium, copper, and Plexiglass liners.

The detector was calibrated using a standard mixed radionuclide solution QCY.46 obtained from Amersham International plc diluted with a carrier solution N.441 to the containers of the same shape and size as the sample vessels. An adjustable shelf, which fits over the detector upon which any combination of six segments can be stacked, was used to increase the distance from the sample vial to the detector as the activity levels increased during the week of experimentation, while maintaining a reproducible geometry (see Figure 4).

3.2 Sampling Procedure

For the sampling procedure of the gas headspace and the reactor container water, it is of particular concern that a representative sample be obtained. It is hoped that during the sample collection the system under study is not radically disturbed. If this is unavoidable, then the system must be disturbed in a consistent manner so that such effects can be corrected for later.

Due to the very low activity levels at the RMC reactor, it was necessary to count the water samples for a minimum of four hours, and the gas samples for eight hours, to be confident that a peak was in fact present. Thus, samples could only be taken twice daily at RMC, and water samples were counted several days after the experiment. At the other reactors, gas and water samples were taken once per hour since 25 minutes was sufficient for good counting statistics.

(a) Gas Sampling

Each SLOWPOKE-2 reactor is equipped with a closed sampling line and pump (5 L/min) for the measurement of any hydrogen in the gas headspace above the reactor water. In order to obtain a uniform and well-mixed fission gas sample before counting, the pump was operated for ten minutes after which it was switched off and the sample counted. At EP, the stir time was varied between one and twenty minutes with no apparent effect upon the measured activity of isotopes with half-lives greater than that of Xe-138. At RMC, a gas sample was obtained with a 50 mL syringe (see Figure 5a) which was inserted into the hydrogen sampling port. For the other reactors, a 44 mL gas chamber (Figure 5a) was connected in line with the pump and the sampling lines were then inserted into the gas headspace to form a closed system.

The transport time from the headspace to the sample chamber was typically less than 30 s.

(b) Water Sampling

The SLOWPOKE-2 reactor water purification system has a bypass loop through which one can obtain samples of reactor container water (see Figure 6). The intake for the sampling pipe is at the top of the water column, approximately 15 cm below the surface, and the reactor water is returned at the level of the core.[2] In obtaining water samples, the pump (which has a flow rate of approximately 10 L/min), was run for two minutes in order to clear the dead space in the sampling line. This stir time was varied at EP between one and five minutes with no noticeable effect upon the concentration of the short-lived fission products. At RMC the water sample was obtained in an open graduated cylinder and then decanted into a Marinelli beaker (see Figure 5b). During this transfer, some degassing had occurred (see Table 2). As such, the sampling procedure was modified for the U of T, EP and KIPF experiments with the use of a sealed, pressurized sample chamber (41 mL) connected in line with the sampling port (see Figure 7). After counting, the sampled water was returned to the reactor container.

3.3 Experiment Description

A brief summary of the operating parameters for each experiment is given in Table 3. The reactor in each experiment was run continuously at one-quarter power, producing a flux of 2.5×10^{11} neutrons/cm^2/s for approximately 100 h to allow the long-lived fission products to reach equilibrium in the reactor. Operation at low power was necessary to maintain excess reactivity. The reactor power history for the various experiments are shown in Figure 8.

The radiation alarm monitor levels were recorded throughout the week so that these levels could be correlated with the fission product inventory in the reactor water. The outlet temperature of the reactor water was also recorded, since the solubility of the noble gases is a function of temperature as is the rate of deposition of the non-volatile fission products. These parameters are also listed in Table 3.

Before the reactor was turned on, the reactor container water was run through the deionizer columns, as per normal weekly maintenance, to remove any fission products present in the water which had been produced during the previous week of reactor operation. A sample of the water was examined and its spectrum recorded. The gas headspace was purged (also part of the weekly maintenance routine) several times until the amount of radioactive isotopes remained constant, and a final spectrum was saved to provide a baseline measurement.

4. EXPERIMENTAL RESULTS AND ANALYSIS

4.1 Concentration Calculation

Typical spectra of the container water from the RMC and U of T reactors are shown in Figures 9a and b, respectively. As can be seen from these figures, the sample from the uranium-aluminum fuelled reactor (U of T) is much more active.

The concentration in the reactor medium (water or gas) of a given isotope as a function of time can be calculated from the gamma ray spectra. In this calculation, the area of the peak of interest is evaluated with the MicroSAMPO analysis program[5] with the use of an energy calibration file, the detector efficiency (see Figure 10), and a shape calibration of the expected photo-peaks. An energy calibration was performed each day of the experiment. The shape calibration file is based on the singlet peaks of one spectrum in an experiment. The peak-search algorithm in MicroSAMPO will search for all peaks of a height which is greater than or equal to a specified number of standard deviations (sigma) of the Compton background. Typical peaks observed in the fission-product spectra were greater than 10 sigma as required for quantitative determination.[6] Peak fits are then performed either automatically or interactively, i.e. a sophisticated peak-area analysis can also be performed for multiplets (overlapping peaks). The count rate for the peak (gammas/s) is calculated by normalizing the peak area by the recorded live time. This information was then incorporated into a Microsoft Excel spreadsheet where the activity concentration of the isotope was calculated given the absolute gamma ray abundance, and the time lag between the collection and measurement of the sample. The decay of the short-lived isotopes during counting was also accounted for in the calculation.

A list of activation and fission products observed in the reactor container water and gas headspace at the U of T reactor are given in Table 4. These isotopes are representative of those observed at all reactors, with the exception of ^{239}Np which was not seen in the water at EP, nor at KIPF. At RMC, this isotope was observed in conjunction with the activation product ^{239}U. Although the radionuclide ^{137}Cs was observed at the deionizer column, it was not identified in the reactor container water because it was obscured by the high Compton background of the short-lived isotopes. The noble gases were the only elements present in the gas headspace of the various reactors, i.e. as measured above the detection threshold limits of the spectrometry system. The alkali metals that were detected in the gas sample chamber were produced from the decay of the noble gases; these fission products had deposited onto the inner surface of the sample vial. In practice, only the noble gases remain as they were created in the reactor container water; consideration of the other fission products, such as the halogens and metals, which may react to form compounds or precipitate out, would greatly complicate the present analysis. Therefore, in this investigation, only the concentrations of the noble gas elements were determined for all of the HEU reactors. Tables and plots of the isotopic concentrations of noble gases as a function of time in the reactor container water and gas headspace have been compiled in Appendix A of the data report (published separately) for the U of T, EP and KIPF reactors.

Concentrations for the other isotopes listed in Table 4 for the higher-burnup reactor at U of T are included in Appendix B of the data report (published separately). In general, for the shorter-lived noble gas isotopes, the concentrations in the reactor medium (water or gas) will increase during reactor operation until an equilibrium has been reached.

The most significant difference between the various reactors is the absolute activity concentrations of the reactor water and gas as shown in Table 2. This table gives the absolute activity concentration of ^{133}Xe after continuous reactor operation at one-quarter power. The activity at the RMC reactor, which is fuelled with uranium dioxide pins, is approximately five orders of magnitude less than that at the U of T reactor which is fuelled with the uranium aluminide pins that have the exposed uranium-bearing end-welds. The fission products observed at RMC are most likely due to surface contamination from the original uranium traces deposited on the fuel pin external surfaces during fuel fabrication.[8,9] Activity levels at U of T are approximately 16 times greater than those at KIPF, which is most likely due to the larger number of flux hours accumulated (see Table 5).

4.2 Transport Time Estimate

There is a delay between the creation of fission products in the core and their uptake at the sampling port in Figure 6. During this time, the activity of the short-lived fission products will have decayed, and this effect must be accounted for. The transport time was therefore estimated by rapidly sampling the coolant at the start of a given experiment (i.e. every three minutes) and noting the time lag between the point at which the reactor had reached power and the first occurrence of the short-lived isotope, ^{138}Xe, at the sampling port. (The reactor would generally reach the flux set point in one to two minutes.) Typical values obtained with this method for the various reactors ranged from about three to fourteen minutes (see Table 6). It is important to note that the transport times in Table 6 are probably smaller than those present during routine sampling (see Section 3.2) since there would be an enhanced circulation from pump operation with the rapid sampling procedure. For the following analysis the transport time is taken to be six minutes at U of T and KIPF, and fourteen minutes at EP.

4.3 Release Rate Calculation

In order to determine the mechanism of release from the core, the release rate must be evaluated for the various fission products. Unfortunately, only the activity concentrations can be directly measured. However, based on mass balance considerations in the closed reactor container, the release rates of fission gases from the fuel into the water (R_{fw}), and from the water into the gas headspace (R_{wg}), can be calculated from the activity concentration data.[7] For instance, the net rate of change of the number of atoms with respect to time of a given radioactive isotope in the water (N_w) is

$$dN_w/dt = R_{fw} - \lambda N_w - R_{wg} \qquad (1)$$

where λ is the radioactive decay constant (s^{-1}). Similarly, the mass balance for the inventory in the gas headspace (N_g) is given by

$$dN_g/dt = R_{wg} - \lambda N_g. \quad (2)$$

These inventories are related to the measured activity concentrations (C) as follows:

$$C = \lambda N/V \quad (3)$$

where V is the given volume of water above the core (1380 L) or the volume of the gas headspace (108 L).[2] Hence, using the above relation, Eqs. (1) and (2) can be rewritten as

$$R_{fw} - R_{wg} = V_w \{(1/\lambda)dC_w/dt + C_w\} \quad (4)$$

$$R_{wg} = V_g \{(1/\lambda)dC_g/dt + C_g\}. \quad (5)$$

As can been seen from Eqs. (4) and (5), a knowledge of the concentration and the derivative of the concentration is required for the calculation of the release rate. A computer program (SUMRT) has been developed by Atomic Energy of Canada Limited for similar analysis of in-reactor loop experiments in the NRX reactor.[10] This program uses a cubic spline fit for the data smoothing. Unfortunately this numerical approach leads to an oscillatory behaviour for the release rate (as a consequence of the derivative calculation). In addition, SUMRT is not equipped to deal with a two-part reactor vessel (such as the reactor container water and gas headspace). At RMC, a spread sheet algorithm has therefore been developed (which is compatible with the MicroSAMPO framework) based on a Savitzky-Golay (S-G) method of curve fitting.[11] The S-G method is well suited to a spread sheet format since it involves simple mathematical operations with tabulated data. This method fits a n-th order polynomial to 2m+1 data points (with labels ranging from -m to +m) to give a smoothed value for the central point (m=0). The labels are then shifted over by one data point and a new region is fitted. For curve-smoothing alone, quadratic and third-order polynomial fits yield identical results. The S-G method avoids the oscillatory behaviour of SUMRT because it uses a polynomial for the smoothed concentration curve which can be easily differentiated. Both SUMRT and the S-G method yield identical results for steady-state reactor conditions. Release rates of the noble gases in the reactor container headspace (R_{wg}) for the HEU reactors based on the S-G algorithm are listed in Appendix C of the data report (published separately).

In general, for the noble gas isotopes, the release rates from the fuel to the water (R_{fw}) are much greater than those from the water to the gas headspace (R_{wg}), i.e. $R_{fw} >> R_{wg}$ (see Appendix C). In this case, Eqs. (4) and (5) can be decoupled such that

$$R_{fw} = V_w \{(1/\lambda)dC_w/dt + C_w\},$$

which can be equivalently written as:

$$dC_w/dt = \lambda R_{fw}/V_w - \lambda C_w. \quad (6)$$

If R_{fw} is relatively constant over the course of the experiment, the solution of Eq. (6) is given by

$$C_w(t) = (R_{fw}/V_w)\cdot(1 - \exp\{-\lambda t\}) + C_{wo} \exp\{-\lambda t\}, \quad (7)$$

where C_{wo} is the initial (measured) concentration in the water at the start of the experiment.

Equation (7) was fit to the measured concentration data, using a Marquardt-Levenberg least-squares fitting algorithm.[12] For isotopes with relatively long-lived precursors (e.g. ^{133}Xe and ^{135}Xe), Eq. (7) must be generalized to account for precursor effects in the container water (see the attached Appendix). As shown in Figure 11, the model fit is in excellent agreement with the measured data (see also Appendix A). The values of the fitting parameter R_{fw} for the noble gas isotopes in each experiment are given in Table 7. As discussed above, these values are at least an order of magnitude greater than those determined for R_{wg} in Appendix C.

5. MODEL DEVELOPMENT

When a fission fragment is created from the splitting of a ^{235}U nucleus, it is highly energetic (average kinetic energy of about 80 MeV) and can therefore travel a finite range (~13 μm) before coming to rest in the uranium aluminide fuel meat where it would normally be contained (see Figure 12). If, however, the fission product is created near the surface of some exposed portion of the fuel (such as at the uranium-bearing end weld line), it can be ejected directly into the surrounding coolant. An 80 MeV particle released from the surface of the fuel will come to rest in the coolant in approximately 22 μm. Such a release can therefore occur by direct fission recoil. Alternatively, a fission fragment created deep inside the fuel will lose its kinetic energy within the above range, following which it may slowly migrate or diffuse through the fuel matrix and escape once it reaches the exposed surface.

Since recoil release is an instantaneous process, the release rate (R_{fw}) (in atoms/s) from the fuel pin into the coolant is independent of the half-life of the fission product so that:[8,9]

$$(R_{fw}/Y)_{rec} = \tfrac{1}{4}\mu(\Delta S/V)F, \quad (8)$$

where: $\Delta S/V$ = ratio of the exposed fuel surface to the total volume of the fuel pin (m^{-1})
μ = average fission-fragment range in the fuel (m)
Y = fission yield for a given radionuclide (atoms/fission)
F = fission rate per pin (fissions/s).

A cumulative fission yield (Table 7) is applied in the above equation to account for decay of the precursor fission products also emitted into the coolant.

On the other hand, according to the diffusion model developed by Booth, the release rate (R_{fw}) will depend on the half-life of the isotope such that[14]

$$(R_{fw}/Y)_{dif} = (\Delta S/S)\, 3(D_f'/\lambda)^{1/2}F, \qquad (9)$$

where: $\Delta S/S$ = fractional surface area of fuel exposed to the coolant per rod
D_f' = empirical diffusion coefficient for fission products in the fuel (s^{-1})
λ = radioactive decay constant (Table 7) for a given radionuclide (s^{-1}).

A Booth diffusion model has been employed in the STARS fuel performance code for the prediction of fission gas release in metal fuels.[15] For example, at lower fuel temperatures, re-solution back into the fuel matrix will dominate so that if any gas bubbles are formed they will remain small, and gas release will therefore depend more on the behaviour of single gas atoms rather than on bubbles. [15,16]

A logarithmic plot of the release rate normalized by the fission product yield (i.e R_{fw}/Y) as function of the decay constant (λ) will thus display a flat horizontal line for a recoil process and a slope of -1/2 for a diffusion process.

Figure 13 shows a log-log plot of the normalized release rates (R_{fw}/Y) versus the decay constant (λ) (based on the data given in Table 7) for the U of T, EP and KIPF reactors. As discussed previously (see Section 4.2), the measured release rates for the short-lived isotopes must be corrected for radioactive decay during transport from the reactor core to the sampling port. This calculation is detailed below.

The mass balance equations (4) and (5) apply to the average concentration of each isotope in the reactor container volume. However, for fission products with half-lives on the order of the transport time, an activity concentration gradient will exist in the reactor container such that at a height x above the core, the concentration will be given by:

$$C(x) = C_o \exp\{\lambda x/v\} \qquad (10)$$

where v is the convective-flow velocity, and C_o is the concentration of the fission product at the site of the reactor core. The average concentration in the container water is obtained by integrating Eq. (10) over the height of the water column (L). Defining the time for a fission product to travel from the core to the intake of the sample pipe as T = L/v, the relationship between the concentration at the top of the water column (at the intake pipe) to the average concentration is:

$$C(L) = \langle C \rangle_{av}\, \lambda T \exp\{-\lambda T\}/(1 - \exp\{-\lambda T\}). \qquad (11)$$

Furthermore, some fission products will decay as they travel through the piping to the water-sampling station. The measured concentration C_{meas} will be given by Eq. (11) but multiplied by the factor $\exp(-\lambda t')$ where t' is the transit time in the piping. Therefore, the average

concentration becomes:

$$<C>_{av} = C_{meas}\,[(1 - \exp\{-\lambda T\})/\lambda T]\exp\{\lambda t_{tr}\} \qquad (12)$$

where $t_{tr} = T + t'$ is the total transport time as measured in Table 6. The time t' is estimated to be 15 seconds based on a piping length of 8 meters, for a pipe with an inner diameter of 3/4", and a pump volumetric flow rate of 10 L/min. Hence, the release rates in Figure 13 have been corrected by multiplying by the factor $[(1 - \exp\{-\lambda T\})/\lambda T]\exp\{\lambda t_{tr}\}$.

Using Eq. (8), the R_{fw}/Y for the entire fuel core based on a recoil process of release is given by:

$$R_{fw}/Y = n\,(R_{fw}/Y)_{rec} = c, \qquad (13)$$

where n is equal to the number of defective fuel pins, and c is a constant = $\frac{1}{4}\mu(\Delta S/V)(nF)$. Similarly if both diffusion and recoil are important, Eqs. (8) and (9) yield

$$R_{fw}/Y = n\{(R_{fw}/Y)_{dif} + (R_{fw}/Y)_{rec}\} = a\lambda^{-1/2} + c, \qquad (14)$$

where $a = 3(\Delta S/S)\cdot(D_f')^{1/2}(nF)$. The models in Eqs. (13) and (14) have been fit to the data in Figure 13 for the various HEU reactors. The fitting parameters (a and c) are listed in Table 8 for both models. A flattening of the release curve is observed for the short-lived isotopes in Figures 13 (a), (b), and (c) indicating that recoil is an important release mechanism. For a given reactor, the values of the recoil parameter (c) in Table 8 are quite similar whether or not diffusion is included. The use of a longer transport time (see Section 4.2) will also tend to flatten out the curves, suggesting a dominant recoil process for the short-lived isotopes.

5.1 Dependence of Release on Reactor Power

An alternative method for determining the mechanism of release is to investigate the dependence of the release rate (R_{fw}) as a function of the fission rate (F) (i.e. reactor power). As seen in Eq. (8) for a recoil process, the release rate varies linearly with the fission rate. On the other hand, fission products can also migrate by solid state diffusion at low fuel temperatures, i.e. below 1000°C in ceramic oxide fuel (UO_2), fission product release has been observed to occur by temperature-independent (athermal) diffusion.[17] (Recall that diffusion has also been implicated as a release mechanism in metal fuels.[15]) Radiation-enhanced diffusion rates have been observed at these low temperatures due to the creation of defects in the solid lattice by fission fragments.[18] In this particular case, the diffusion coefficient (D_f') is proportional to the fission rate.[17,18] Hence, inspection of Eq. (9) reveals that the release rate should vary as $F^{3/2}$. At higher fuel temperatures, the diffusion coefficient will vary as an Arrhenius function of temperature, implying a stronger dependence on the reactor power.[19]

For this investigation, the isotope, ^{138}Xe, was selected for monitoring (in the KIPF reactor) since its half-life of 14.6 min is sufficiently short to allow it to reach equilibrium conditions quickly in the container water at each power level (see Figure 8). On the other hand, its half-life is large enough that it is not unduly sensitive to transport time effects which are also power dependent (see Table 6). A linear variation of the release rate of ^{138}Xe (corrected for decay during transport) with reactor power is shown in Figure 14. Similar results were also observed for the U of T and EP reactors. As discussed above, this dependence is indicative of recoil.

In conclusion, recoil constitutes a significant portion of the release mechanism from the fuel to the coolant since:

i) the (R_{fw}/Y) versus λ plots show a dominant recoil release component for the short-lived isotopes;

ii) the release rate of ^{138}Xe is linear with reactor power;

iii) the model in Eq. (7) is in excellent agreement with the concentration data; in the development of the model, a constant release rate was assumed that is consistent with a recoil process [Eq. (8)] for a constant power level (see attached Appendix).

6. FUEL-SURFACE EXPOSURE

The average fuel exposure per pin can be determined by employing the recoil model in Eq. (13), where for a cylindrical pin of radius r and length ℓ:

$$R_{fw}/Y = \tfrac{1}{4}\mu(\Delta S)\,F_c/(\pi r^2 \ell) = c. \qquad (15)$$

Assuming that all pins are contributing to the release, the parameter F_c $(=n \cdot F)$ can be estimated from the average fission rate for the core. If the reactor is operating at 5 kW, and each fission event liberates 200 MeV of energy, then F_c is equal to 1.56×10^{14} fissions/s. The range (μ) of the fission fragment in the uranium aluminide fuel is calculated as follows. Most of the noble gases in the coolant are due to the decay of precursor fission products. The "mean" precursors for krypton and xenon can be obtained by weighting the mass and atomic numbers of all of the precursors with their direct fission yields. For krypton and xenon, respectively, ^{88}Br and ^{135}I can be considered as the primary fragments.[20] The fuel alloy can be represented by the empirical formula $UAl_{22.4}$, which corresponds to the average density given in Table 1 for small particles of UAl_4 dispersed in aluminum. As shown in Table 9, the ion ranges in the alloy can be determined from the ranges in the individual elements of the alloy, and the Bragg combining law for the compound.[21,22] This calculation is in good agreement with that determined by the TRIM (TRansportation of Ions in Matter) code.[23] The average range of a fission fragment in the fuel alloy is therefore estimated to be

~13 μm. Using the fuel pin dimensions in Table 1, and the values of c (recoil/diffusion model) in Table 8, the fuel exposure ΔS (per pin) can be determined from Eq. (15). The result of this calculation is plotted in Figure 15 as a function of the flux-hours accumulated at the end of the experiment for the HEU reactors (Table 5). As can be seen from this figure, the exposed area has been increasing with usage (i.e. burnup). The increase in the fission-product release is associated with the core burnup rather than the physical age of the reactor. This is apparent from a comparison of the radiation levels at the U of T and University of Alberta (U of A) reactors. Although both SLOWPOKE-2 reactors were commissioned at about the same time, the lower-burnup core at U of A (42,236 x 10^{11} n cm^{-2} s^{-1} - hours) has substantially lower radiation levels; for example after 4 h of operation at full power, the U of A levels are 9 mrem/h[24] compared with 40-100 mrem/h at U of T. A semi-log plot in Figure 15 is justified by the observed increase of the Xe-133 concentration in the reactor container water at Ecole Polytechnique with the accumulated flux-hours as shown in Figure 16.[25]

The curve in Figure 15 also correlates well with the reactor alarm monitor levels given in Table 3 for the various reactors. Hence, the monitor levels serve as an indication of the "normal" progression of the fission product release and exposed fuel surface area. The reactor alarm monitor levels listed were reached within six hours of operation (at one-quarter power), and remained relatively steady over the course of the experiment, i.e. for a period of operation of about 100 h. It may be possible to obtain an estimate of the condition of the other HEU reactors by running them at one-quarter power, and comparing the alarm levels reached with those in Figure 15.

The same curve can also be extrapolated back to zero burnup to determine the amount of fuel exposure for the unirradiated fuel. This extrapolation implies that an average (as fabricated) pin (see Figure 1) would have ~ 10 mm^2 of fuel exposure; the uncertainty in this extrapolation yields a range of 4 to 20 mm^2. This value can be compared to a metallographic examination of archive fuel elements.[26] As seen in Figure 17a, large voids are generally present at the weld zone in the aluminum cladding. A cross section of the weld zone (Figure 17b) also reveals numerous voids, i.e. the largest void dimension is about 1.7 mm long x 0.3 mm high. A band is seen at the end weld line of the fuel pin after excess uranium-bearing material had been removed by machining (see Figure 1b). Based on the metallographic examination, the average exposed fuel surface is estimated to be 4.0 mm^2.[26] This value is in good agreement with that determined from the fission-product release analysis (10 mm^2). The estimate from the metallographic examination is a lower-bound value since one must consider the total surface area rather than the geometrical one due to the presence of any surface irregularities.

The extrapolated value would increase in the above calculation if it were assumed that not all of the fuel pins were defective or if the uranium-bearing band was depleted in uranium (i.e. as a consequence of the discharge weld process which would have mixed the aluminum sheath material with the uranium alloy fuel meat).

A small increase in the release of fission products may also be attributed to a flattening of the flux profile with increasing core burnup. As seen in Figure 18, the axial flux distribution is relatively constant and does not change by more than a factor of 1.4 over the core height. The flux at the top of the fuel cage is quite close to the axially-averaged value because of the influence of the Be reflector. A reactor physics study[27] using the TRIVAC code for the EP core indicates that at its present level of burnup, the value of the thermal flux at the position of the end welds is also very close to the average value throughout the core. Although the flux profile is skewed to the bottom of the core because of the presence of the control rod, the addition of Be at the top of the core during reshimming (i.e. from 1/2" to 2") slightly increases the flux at the upper weld line. However, the flux redistribution in Figure 18 cannot account for the order of magnitude increases in release as observed in Figure 15.

Since the recoil component of the fission product release has been increasing with core burn-up, it is apparent that a larger surface area of uranium-bearing material is being exposed to the coolant by some continuous process, such as corrosion. Corrosion would most likely occur at the contaminated end welds of the fuel pins, i.e. the uniform corrosion rate of the aluminum cladding is small enough (0.76 - 1.53 μm/yr at operating temperatures) that it should remain intact throughout the core lifetime.[26] The presence of impurities such as copper or chloride ions would accelerate the corrosion of the cladding;[28] however, weekly conductivity measurements and gamma ray spectroscopy suggest that these ions are not present in the reactor container water. Unfortunately, limited data are available on the corrosion behaviour of uranium-aluminum alloys under conditions similar to those in the SLOWPOKE-2 reactor.[16,29,30] Aqueous corrosion and the washing-out of uranium-aluminum alloy fuel at a rate of 14 g/year was observed in the Advanced Test Reactor (ATR) after the formation of a pit defect in the plate-type fuel.[29] However, the coolant flow and temperature of the cladding of the ATR fuel were higher than those associated with the SLOWPOKE-2 reactor, both of which dramatically increase the corrosion rate.[29] The corrosion rate of the uranium-aluminum alloy has been estimated to be two to three times that of the aluminum cladding.[26] Corrosion at the end-weld line could increase any surface irregularities thereby exposing more uranium-bearing material to the coolant.

7. VISUAL EXAMINATION OF THE EP CORE

A visual examination of the SLOWPOKE-2 core at EP was performed on 24 September 1991 in conjunction with a reshimming operation. This reactor has the second highest burnup of the HEU reactors in Table 5. A visual examination could not be performed at the higher-burnup reactor at U of T because of the installation of a permanent Be doughnut. In preparation for this examination the Be shim plates and tray were removed. The core was then lifted out of its resting position so that its entire length was exposed. A remote underwater television camera Westinghouse Model ETV 1250 with built-in light source and right-angle viewing attachment (see Figure 19) provided by Chalk River Laboratories (CRL), was lowered down beside the core. Direct observation of the entire outer ring of fuel pins and portions of some inner pins was possible. A Commodore Model 1802 Video Monitor

was used to view the operation, and the images were recorded in black and white with a Canon Video Recorder Model VR-40 on VHS tape.

The important observations of this examination are summarized below:

(i) several fuel pins had "pimple-like" bumps (Figure 20a),

(ii) one inner pin appeared to have a short vertical split (5mm long by 1 mm wide), although this observation may have been an artifact of the lighting since this feature was not observed following a second visual pass of the core,

(iii) some swelling of the bottom section of ten to twelve peripheral fuel pins and three to four inner pins, was observed extending over 15 mm from the machined weld zone; the maximum diameter increase of the area is about 10 to 15% (Figure 20b),[26]

(iv) superficial defects were observed on a number of pins, e.g. scratches (which probably resulted during the extrusion process or during the machining of the weld areas), as well as some slight discolorations,

(v) the end welds of the fuel pins were visible with no significant evidence of corrosion (although the resolution capability of the camera and lighting were limited) (Figure 20c).

In summary, the core appeared to be in good condition with no evidence of gross failure, or any loss of structural integrity. A videotape copy of the core examination is available at RMC.

Based on this examination, it can be shown that the "bumps" are not the primary source of the fission product release. During the visual examination, the outer-halves of the fifty-three fuel pins on the circumference of the fuel cage were examined in detail along approximately two-thirds of their length. Four of these fifty-three pins had a single "bump", typically 1 mm in diameter on the surface of the cladding. If the portion viewed constitutes a representative sample of all 296 fuel pins, then one would expect a *total* surface area coverage of 53 mm^2. On the other hand, the fission product analysis indicates an exposed fuel surface *per pin* of ~ 50 mm^2 for the EP core (Figure 15), for a total area of $\sim 14{,}000$ mm^2. This latter value is orders of magnitude greater than the area covered by the bumps. In addition, there is no evidence to suggest that the bumps are cracked, exposing the underlying fuel surface. Therefore, it is more likely that the source of the activity release is from the exposed end welds.

A hot cell examination of a few spent fuel pins should therefore be performed at CRL after the decommissioning of the KIPF reactor so that the weld areas, and possible swelling of the cladding can be metallographically examined.

8. CONCLUSIONS

(i) Highly enriched uranium (HEU) fuel elements for the SLOWPOKE-2 reactors have a band of uranium-bearing material (at the end-weld line) exposed to the coolant as a consequence of the fuel fabrication process. This band of exposed fuel is the initial source of fission products in the reactor container water.

(ii) Fission-product activity levels have been quantitatively measured by gamma spectroscopy methods in the reactor container water and gas headspace of SLOWPOKE-2 reactors fuelled with uranium alloy cores at the University of Toronto (U of T), Ecole Polytechnique (EP) and Kanata Isotope Production Facility (KIPF). Activity levels in the SLOWPOKE-2 reactor at the Royal Military College (RMC) (containing a uranium dioxide core) have also been measured as part of the commissioning test of the spectroscopy system.

(iii) The predominant radionuclides observed in the reactor container water after approximately 100 hours of operation at 5 kW include: the noble gases; and the alkali metals, cesium and rubidium. These metals are produced principally from the decay of the noble gases. Iodine and molybdenum were also observed. Only noble gases are believed to be present in the gas headspace of the reactor container.

(iv) The release of the shorter-lived noble gases from the HEU alloy cores to the reactor container water is due predominantly to a recoil process, with an additional component of release due to diffusion for the longer-lived isotopes. This study suggests that increased activity levels with time can be attributed to corrosion of the end weld area. The initial exposed surface area determined from the fission product release study is consistent with the results of a metallographic examination of several unirradiated fuel pins.

(v) The extremely low levels of fission products measured at the low enriched uranium (LEU) fuelled reactor at RMC are due to tramp uranium contamination on the surface of the Zircaloy cladding. By way of comparison, the ^{133}Xe levels were five orders of magnitude less than those measured at U of T.

(vi) The measured alarm monitor levels and fission-product activities correlate with the burnup of the various HEU reactors. The exposed fuel surface area has increased by an order of magnitude with burnup in the U of T core.

(vii) An underwater visual examination of the outer fuel elements of the EP core was performed. The core appeared to be in good condition with no evidence of deterioration (gross failure), or any loss of structural integrity. Approximately four of the 53 peripheral pins examined contained a small bump, and ten to twelve pins exhibited swelling (10 to 15%) predominantly at the bottom end of the pins. No evidence of corrosion of the cladding was observed.

(viii) No fission products were detected in the pool water. In addition, the release of fission products into the reactor container water and gas headspace poses no immediate health or safety hazard.

9. RECOMMENDATIONS

The following actions are recommended:

(i) A consistent set of alarm trip points needs to be established based on the experience gained in this study. The alarm monitors should remain capable of detecting increases in radiation due to power transients or loss of pool water shielding.

(ii) The condition in the other HEU-fuelled reactors should be examined by running these reactors at one-quarter power, and comparing the alarm levels reached after six hours (at their given core burnup) with those in Figure 15.

(iii) A quantitative determination of the uranium concentration at the weld line of several unirradiated fuel elements should be performed using energy dispersive x-ray (EDX) analysis.

(iv) A hot cell examination of several spent fuel pins should be considered (i.e. when available from the KIPF reactor which will be decommissioned shortly). This metallographic examination could provide further information on the corrosion of the end-weld areas and the possible cause of the bumps and fuel swelling.

Table 1: A Comparison of the HEU and LEU SLOWPOKE-2 Cores[a]

	HEU Core (U of T, EP, KIPF)	LEU Core (RMC)
Fuel:		
Material	28 wt% U 72 wt% Al (UAl_4 in Al)	UO_2
Enrichment (wt% ^{235}U in U)	93	19.89
Radius (mm)	2.11	2.083
Fuel Stack Length (cm)	22.0	22.7
Density (Mg/m^3)	3.40	10.6
Specific Heat ($J\ kg^{-1}\ K^{-1}$)	683	236
Thermal Conductivity ($W\ m^{-1}\ K^{-1}$)	171	4.67
Sheath:		
Material	Al-1050	Zircaloy-4
Outside Radius (mm)	2.62	2.63
Thickness (mm)	0.51	0.51
Density (Mg/m^3)	2.7	6.55
Specific Heat ($J\ kg^{-1}\ K^{-1}$)	903	290
Thermal Conductivity ($W\ m^{-1}\ K^{-1}$)	238	12.6
Core Description:		
Total Mass of ^{235}U (kg)	0.87	1.12
Number of Pins	317 (KIPF) 296 (EP) 298 (U of T)	198

(a) Taken from References 1 to 4.

Table 2: ^{133}Xe Concentration in Reactor Container Water and Gas Headspace (5 kW)

Reactor	Xe-133 Concentration[a] (MBq/L)		Time After Start-up (h)
	Water	Gas	
RMC	1.9×10^{-5} [b]	1.4×10^{-5}	92
KIPF	0.08	0.06	72
EP	0.68	0.34	72
U of T	1.4	2.5	72

(a) The typical error is less than 10%.

(b) Due to possible degassing during sampling, the actual concentration of ^{133}Xe may be larger.

Table 3: Summary of SLOWPOKE-2 Fission Product Experiments

Reactor	Date of Experiment	Test Description	Reactor Power (kW)	Radiation Monitor Levels (mR/h)			Coolant Outlet Temp (^{o}C)	Coolant pH
				Reactor	Deionizer (prestart-up)	Area		
RMC	5-9 Nov 90	Constant operation at 1/4 power	5	N/A	N/A	N/A	N/A	N/A
U of T	26-30 Nov 90	Constant operation at 1/4 power	5	8 - 10	N/A	0.08	28 - 33	N/A
	20-21 May 91	Transport time calculation at 1/4 power;	5	N/A	N/A	N/A	N/A	N/A
		Transport time and operation at full power.	20	40-100 (level recalibrated in Mar 91)	N/A	0.08 - 0.1	40 - 45	N/A
EP	25 Feb - 1 Mar 91	Transport time calculation;	5	N/A	4 - 6	N/A	27	N/A
		steady operation at 1/4 power;	5	2 - 3		0.05 - 0.1	27 - 34	
		Power ramp at end of test.	5	2 - 3		0.05 - 0.1	27 - 34	
			10	6		0.06 - 0.1	35 - 42	
			20	8 - 20		0.1 - 0.2	51 - 54	
KIPF	9 - 11 Apr 91	Transport time calculation;	5	0.4 - 0.6	2 - 4	0.4	24 - 28	N/A
		Power ramp at 1/4, 1/2, 3/4, and full power.	5	0.6 - 1.0		0.2 - 0.4	29 - 32	N/A
			10	2 - 4		0.4 - 0.6	36 - 41	N/A
			15	N/A		N/A	45 - 47	N/A
			20	2 -6		1 - 2	40 - 46	N/A
	13-17 May 91	Constant operation at 1/4 power;	5	0.8 - 1.5	4 - 6	0.4 - 0.6	28 - 39	5.5 - 6

N/A: Not Available

Table 4: Observed Radionuclides at the University of Toronto

A. Reactor Container Water	
Fission Products	
Noble Gases:	Kr-85m, -87, -88, -89 Xe-133, -133m, -135, -135m, -137, -138
Halogens:	I-131, -132, -133, -134, -135
Alkali Metals:	Rb-88, -89, Cs-138
Alkaline Earths:	Sr-91, Ba-140
Noble Metals:	Mo-99, Tc-99m
Rare Earths:	Y-91m, La-140, -142, Ce-141, -143, Nb-95, Zr-95
Activation Products	
Noble Gases:	Ar-41
Alkali Metals:	Na-24
Actinides:	Np-239
B. Gas Headspace[a]	
Fission Products	
Noble Gases:	Kr-85m, -87, -88, -89, -90 Xe-133, -133m, -135, -135m, -137, -138
Alkali Metals:	Rb-88, -89, Cs-138
Activation Products	
Noble Gases:	Ar-41
C. Deionizer Column[b]	
Halogens:	I-131
Alkali Metals:	Cs-137
Alkaline Earths:	Ba-140
Rare Earths:	La-140, Nb-95, Zr-95

(a) The alkali metals result from the radioactive decay of the noble gas species in the sample vial.

(b) Based on a previous gamma spectroscopy analysis.[7]

Table 5: **Post-test Burnup of the SLOWPOKE-2 Reactors**

Reactor	Burnup[a] (x 10^{11} n cm^{-2} s^{-1} - hours)
University of Toronto	112,643
Ecole Polytechnique	81,381
Kanata Isotope Production Facility	29,939
Royal Military College	30,988

(a) Units given in flux-hours. Significant digits reported as per reactor log.

Table 6: Transport Time from the Reactor Core to the Sampling Port[a]

Reactor	Transport Time, t_r (min)	
	(5 kW)[b]	(20 kW)[b]
KIPF	3 - 6	
EP	11 - 14	
U of T	3 - 6	2.5 - 4.5

(a) Based on the measurement of ^{138}Xe (see text).

(b) Transport time measured at a given reactor power.

Table 7: Release Rates from the Fuel to the Container Water (R_{fw}) for the U of T, EP and KIPF Reactors

Isotope	Decay Constant, λ (s^{-1})	Fission Product Yield[a], Y (%) (atoms/fission)	Release Rate[b], R_{fw} (x 10^8 atoms/s) (errors reported to 1 standard deviation)		
			U of T	EP	KIPF
^{85m}Kr	4.31×10^{-5}	1.31	5.82 ± 6.6%	2.65 ± 6.8%	0.770 ± 6%
^{87}Kr	1.48×10^{-4}	2.52	7.99 ± 10%	3.52 ± 7.1%	1.32 ± 7.4%
^{88}Kr	6.89×10^{-5}	3.55	9.88 ± 6.7%	4.29 ± 7.1%	1.38 ± 7%
^{89}Kr	3.61×10^{-3}	4.60	2.94 ± 10%	N/A	0.638 ± 11%
^{133}Xe	1.52×10^{-6}	6.70	38.6 ± 10%	26.2 ± 8.5%	4.76 ± 9.9%
^{133m}Xe	3.56×10^{-6}	0.195	1.15 ± 22%	N/A	0.445 ± 40%
^{135}Xe	2.12×10^{-5}	6.54	29.4 ± 7%	14.4 ± 6.2%	3.91 ± 6.5%
^{135m}Xe	7.42×10^{-4}	1.21	2.14 ± 6%	0.606 ± 7.4%	0.233 ± 46%
^{137}Xe	2.75×10^{-3}	6.06	3.81 ± 10%	N/A	0.506 ± 18%
^{138}Xe	7.97×10^{-4}	6.42	11.6 ± 6.5%	3.26 ± 6.4%	2.03 ± 8.2%

(a) Based on ENDF/B-V Data (Taken from Reference 13.)

(b) This calculation assumes that V_w = 1380 L (Reference 2, p. 3.4). The release rate for ^{133m}Xe is based on water samples taken at the end of the experiment to allow for the decay of the short-lived isotopes.

Table 8: Fitting Parameters of Fission-Product Release Models[a]

Reactor	Recoil Model[b]	Recoil and Diffusion Model[c]	
	c (fissions/s)	a (fissions/$s^{1/2}$)	c (fission/s)
U of T	$2.7 \times 10^{10} \pm 17\%$	$6.3 \times 10^{7} \pm 25\%$	$2.0 \times 10^{10} \pm 17\%$
EP	$1.3 \times 10^{10} \pm 24\%$	$4.5 \times 10^{7} \pm 22\%$	$7.7 \times 10^{9} \pm 23\%$
KIPF	$4.2 \times 10^{9} \pm 17\%$	$7.2 \times 10^{6} \pm 44\%$	$3.3 \times 10^{9} \pm 22\%$

(a) Using T = 6 min, 14 min (see Table 6). Errors are quoted to one standard deviation

(b) See Equation 13.

(c) See Equations 14.

Table 9: Calculation of Fission-Fragment Range in Uranium Alloy Fuel

Ion	Energy (MeV)[a]	Range (mg/cm²)			Range (μm)[d]	
		U[b]	Al[b]	$UAl_{22.4}$[c]	$UAl_{22.4}$	$UAl_{22.4}$ (TRIM)
Br-88	100	15.9	4.23	5.32	15.6	15.5
I-135	67	11.5	2.93	3.70	10.9	11.9
				Average:	13.3	13.7

(a) It is assumed that Br and I fragments carry 100 and 67 MeV of the available fission energy (see Reference 20).

(b) Range data has been taken from Reference 21.

(c) Based on Bragg law in Reference 22.

(d) Assumes a density of 3.4 Mg/m^3 for the uranium alloy.

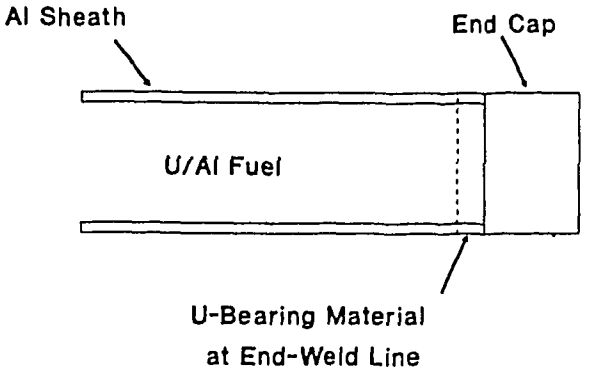

(a)

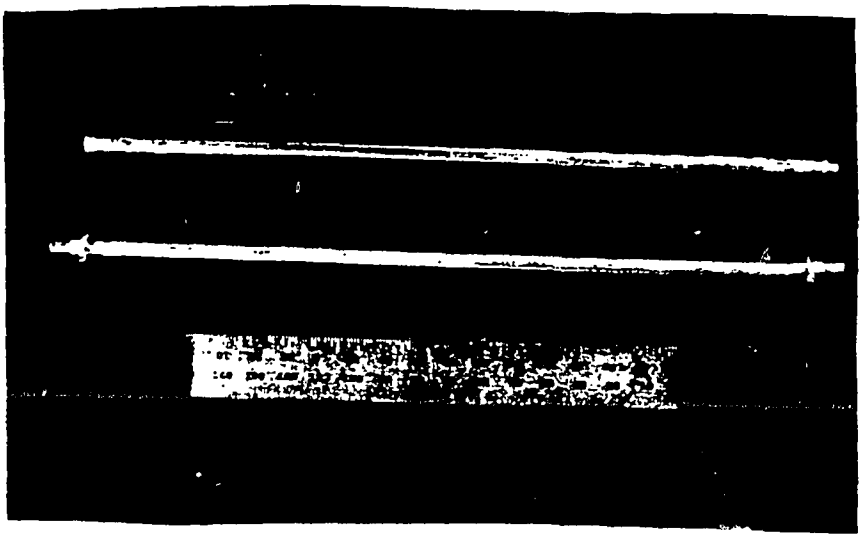

(b)

Figure 1: (a) Schematic diagram of the uranium aluminide fuel pin showing the location of the exposed fuel.

(b) Photograph of the SLOWPOKE-2 uranium aluminide fuel pin as welded (bottom) and with the final machined end caps (top). (Courtesy of Atomic Energy of Canada Limited.)

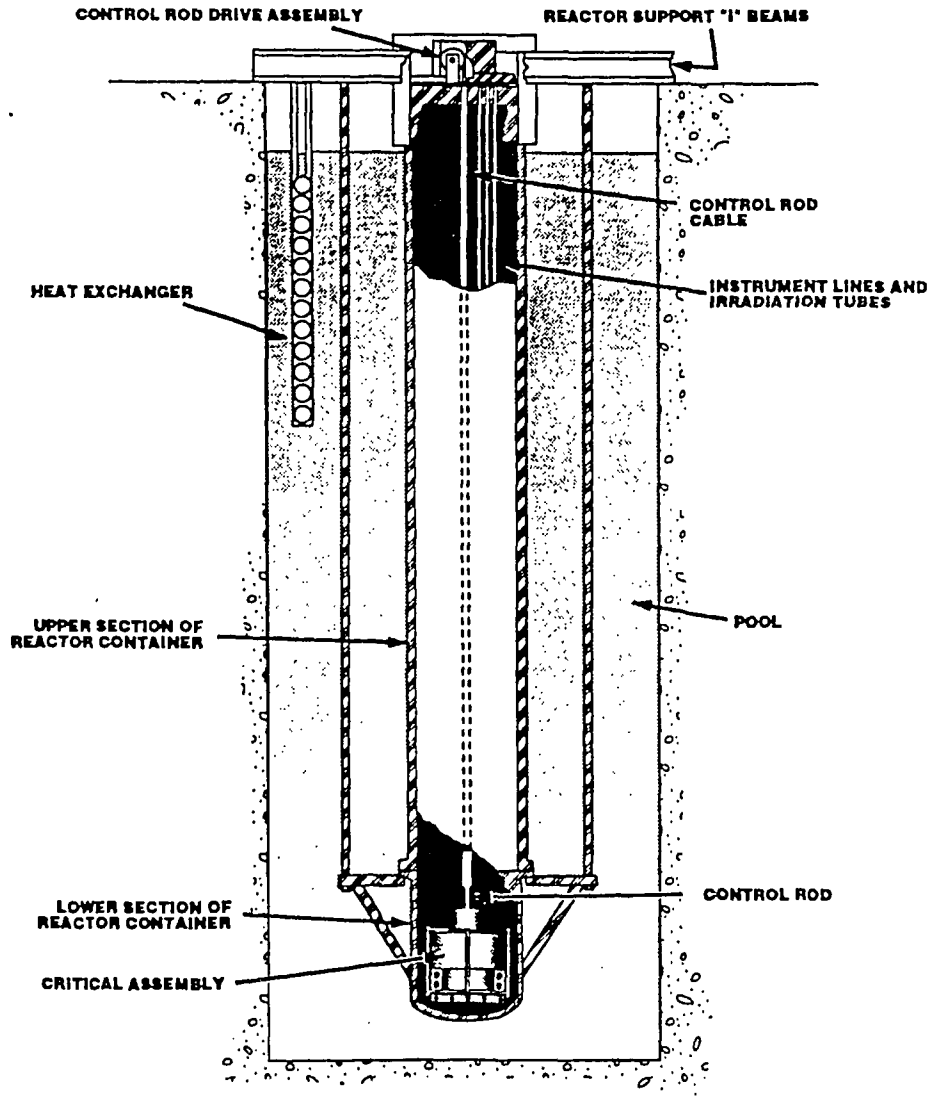

Figure 2: Reactor general assembly. (Taken from Reference 2.)

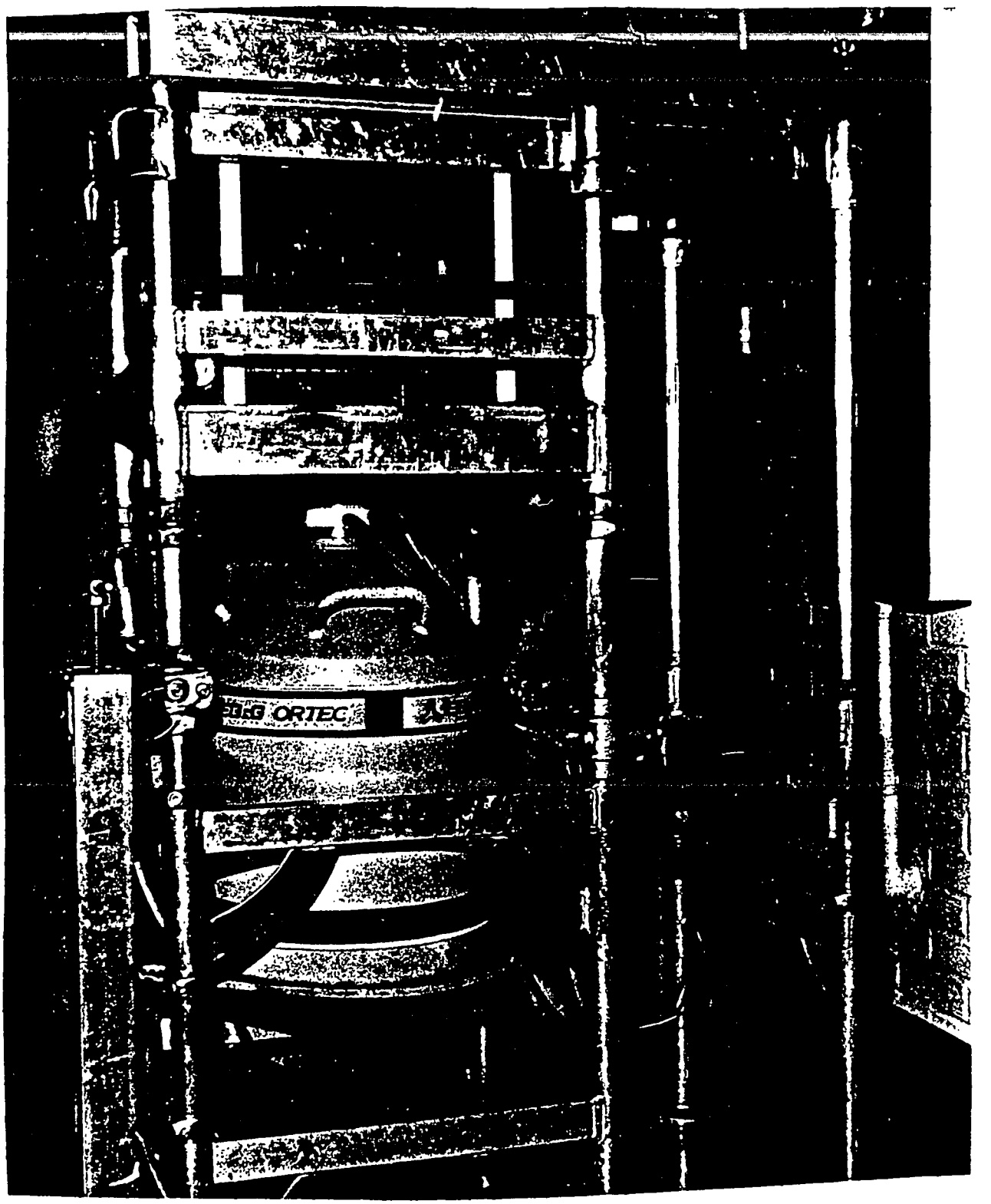

Figure 3: Transportable lead shielding with the GMX detector in place.

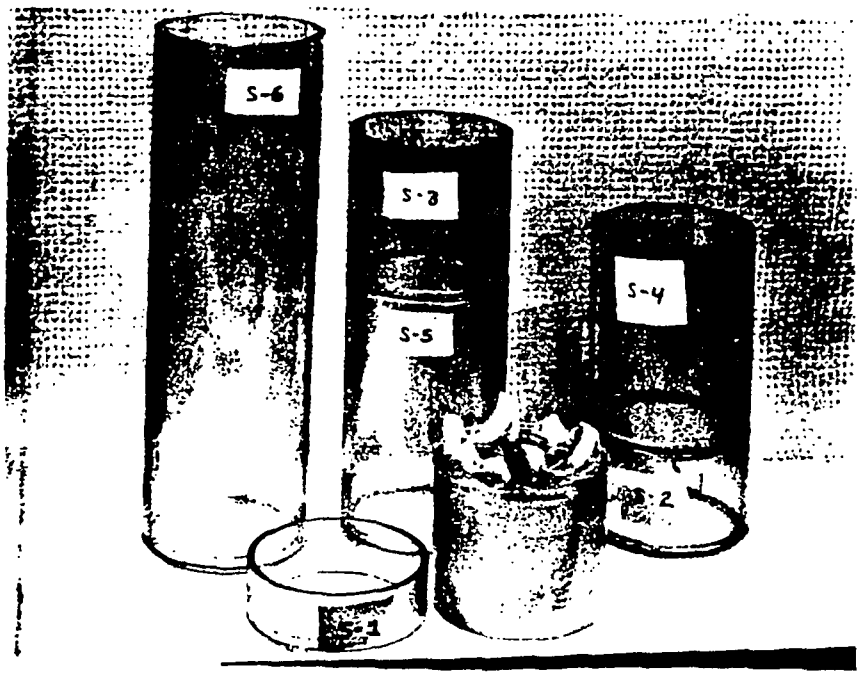

Figure 4: Adjustable segmented shelf. The curved base plate for the syringes and cylindrical sample holder (see Figure 5) is shown in the foreground.

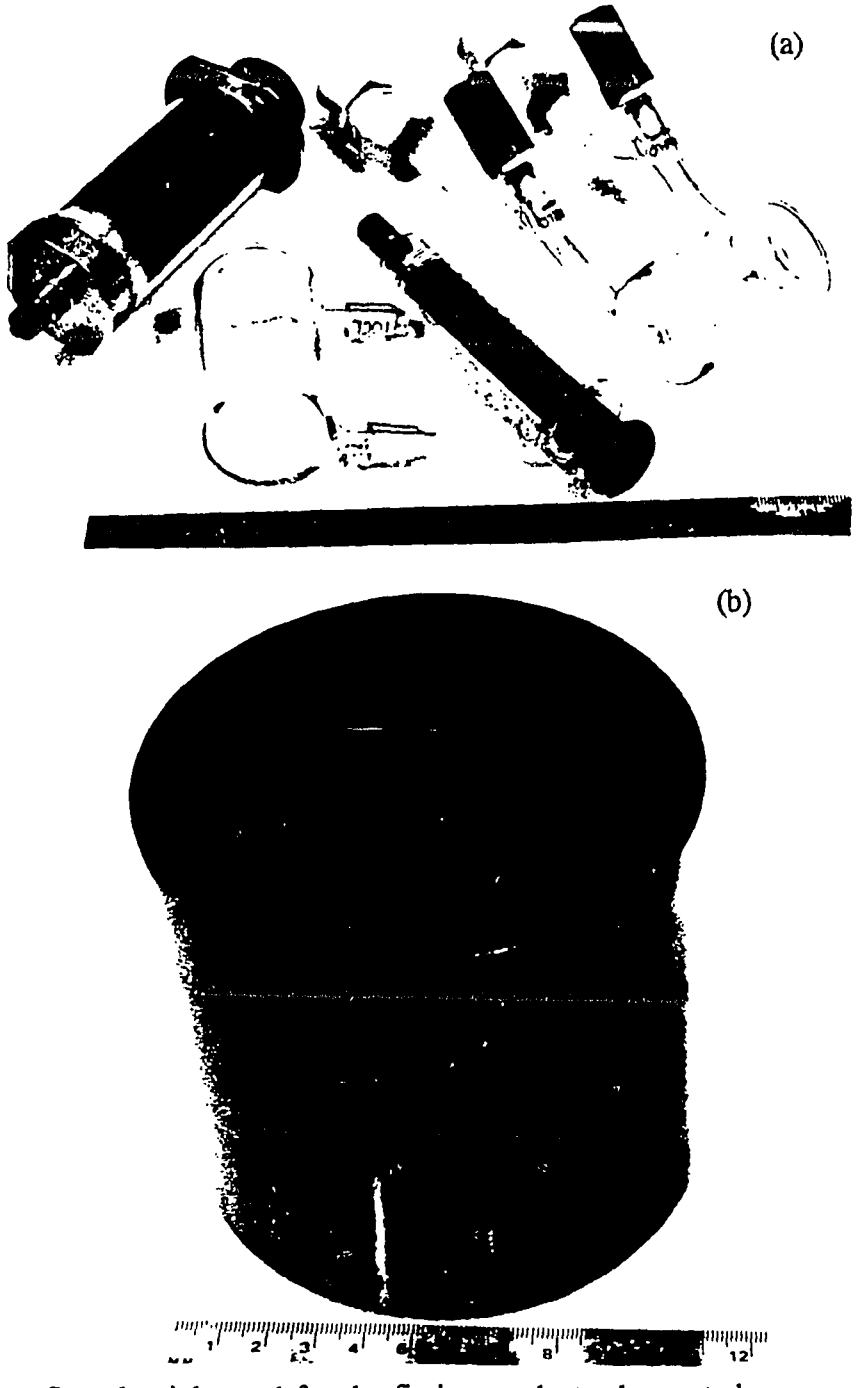

Figure 5: Sample vials used for the fission-product release study.

(a) Assorted sample vials, left to right: A) 50 mL gas-tight syringe; B) 44 mL gas sample chamber; C) 10 mL gas-tight syringe; D) 41 mL sealable water chamber.

(b) A 500 mL-capacity polyvinyl chloride Marinelli beaker used for water samples at RMC.

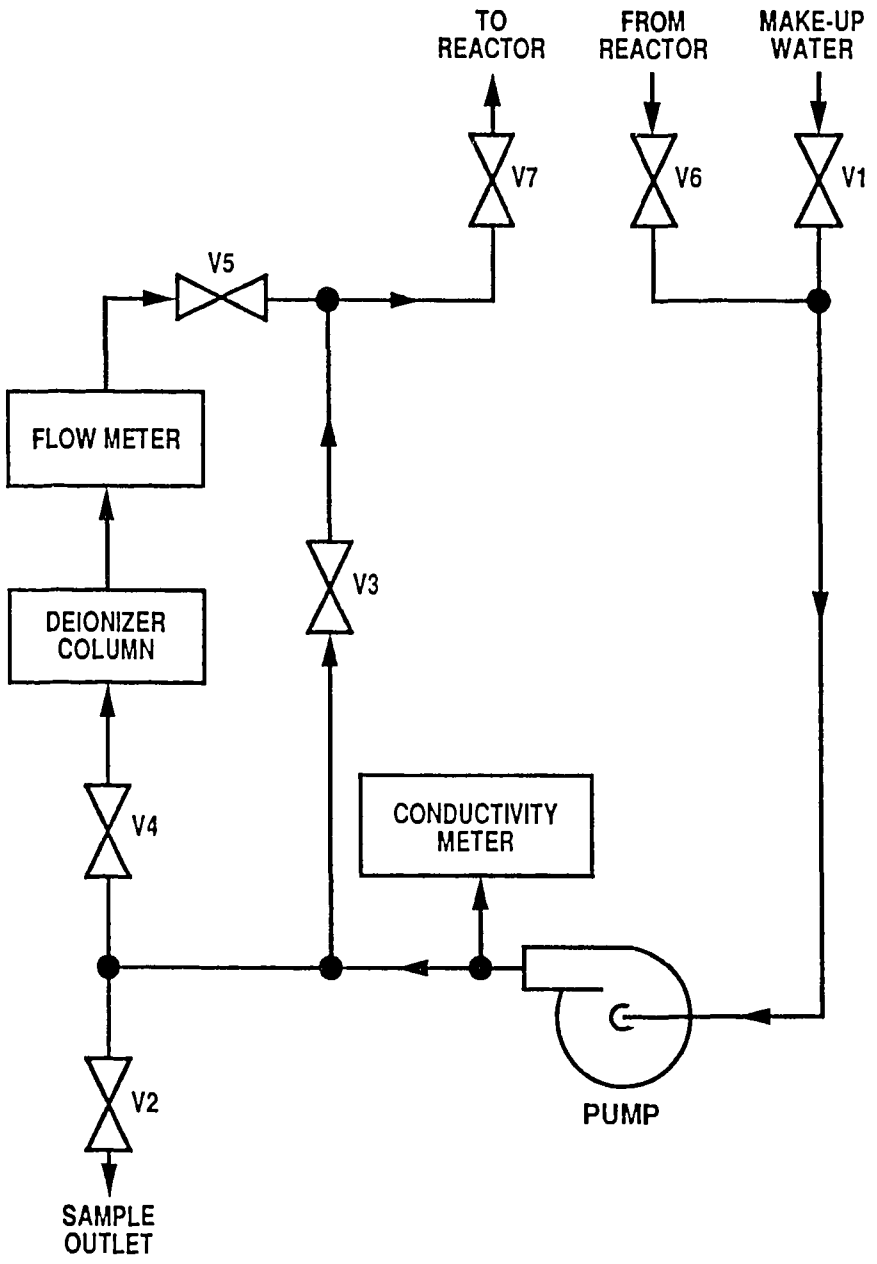

Figure 6: Reactor container water flow diagram.

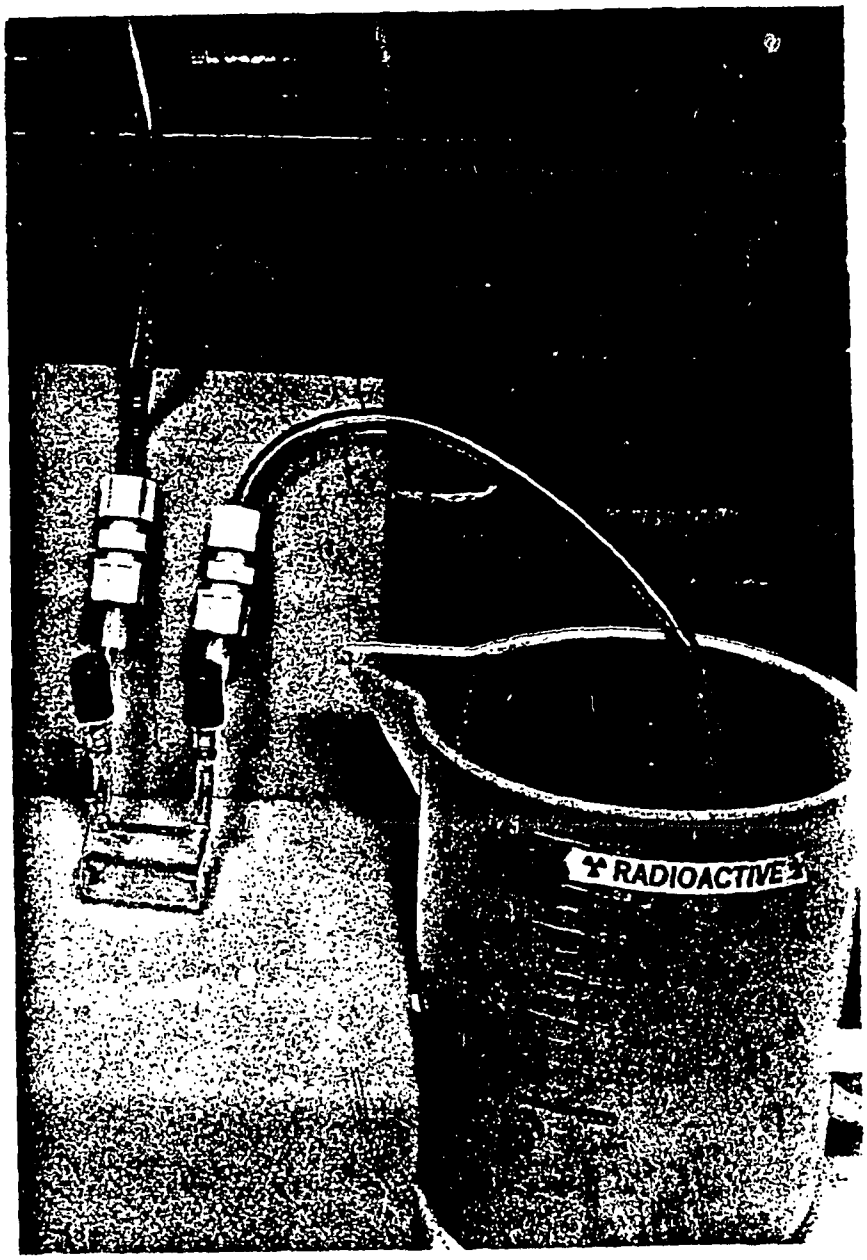

Figure 7: Connection of the reactor container water sample to the sampling port.

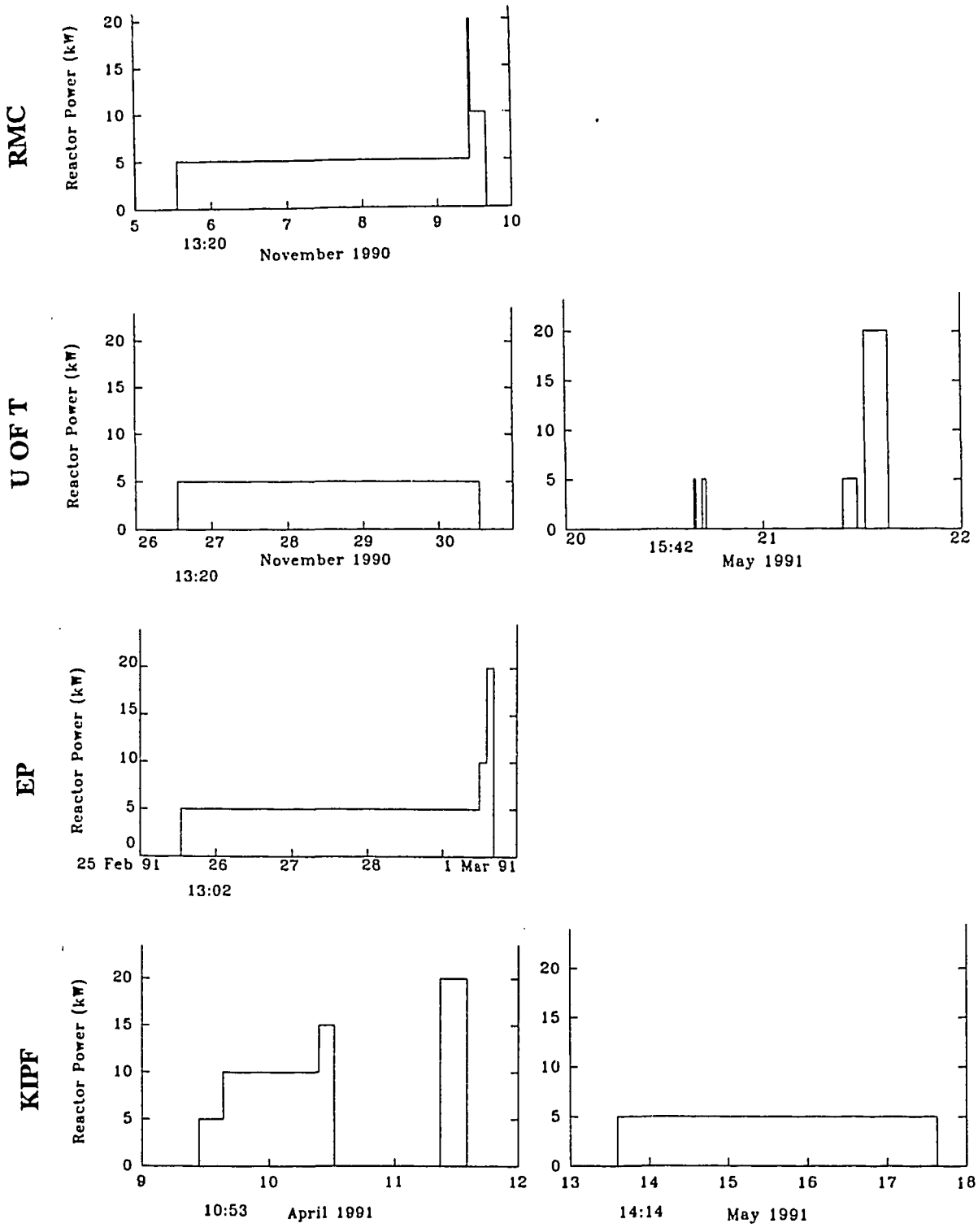

Figure 8: Reactor power history for SLOWPOKE-2 experiments.

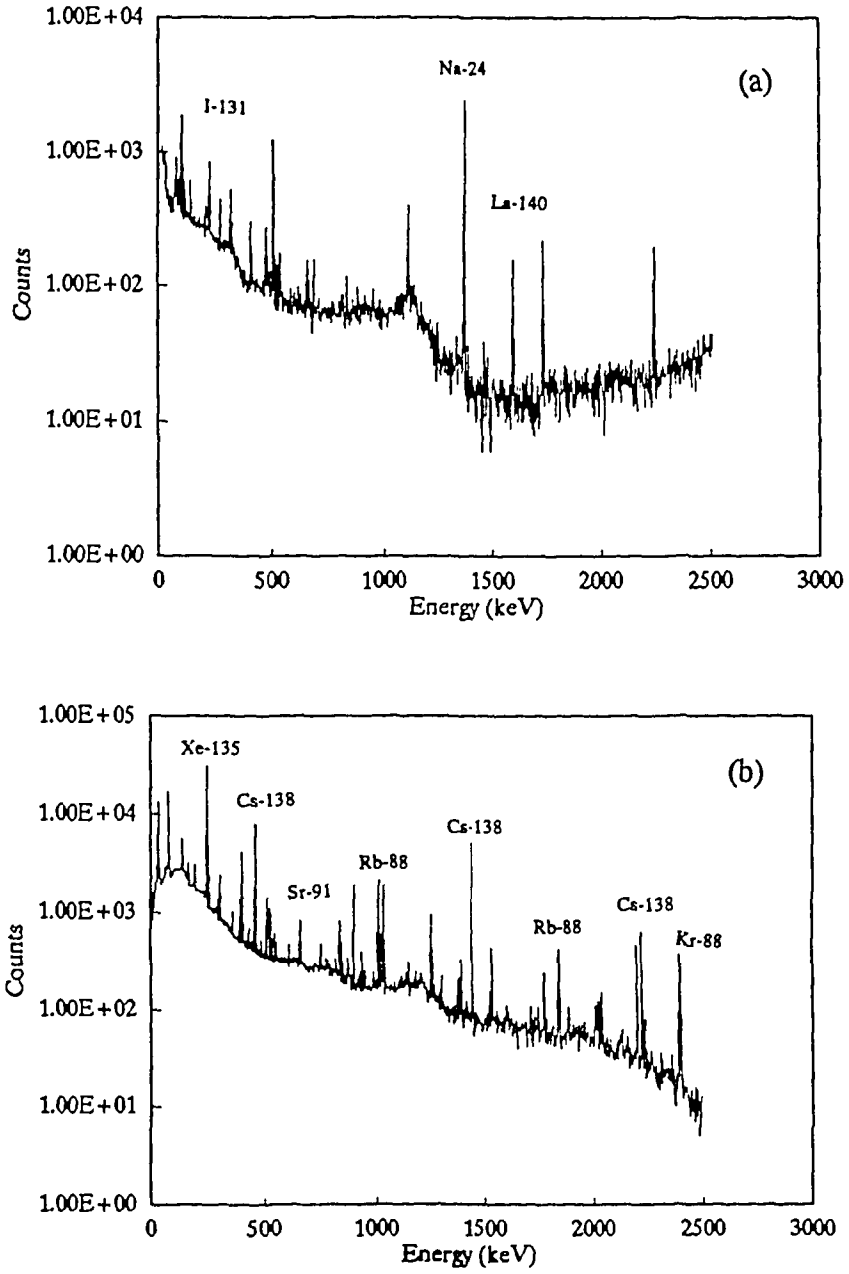

Figure 9: Gamma ray spectrum for the reactor container water.

(a) Spectrum of a 350 mL sample counted for 12 h at RMC.
(b) Spectrum of a 41 mL sample counted for 10 min at U of T.

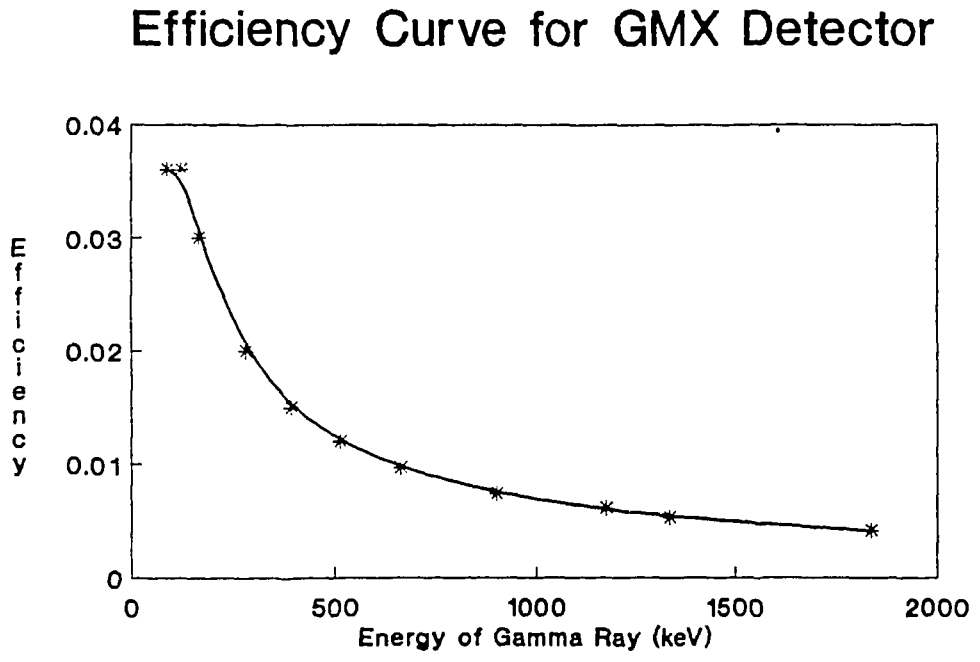

Figure 10: Detector efficiency curve for the GMX high purity germanium detector.

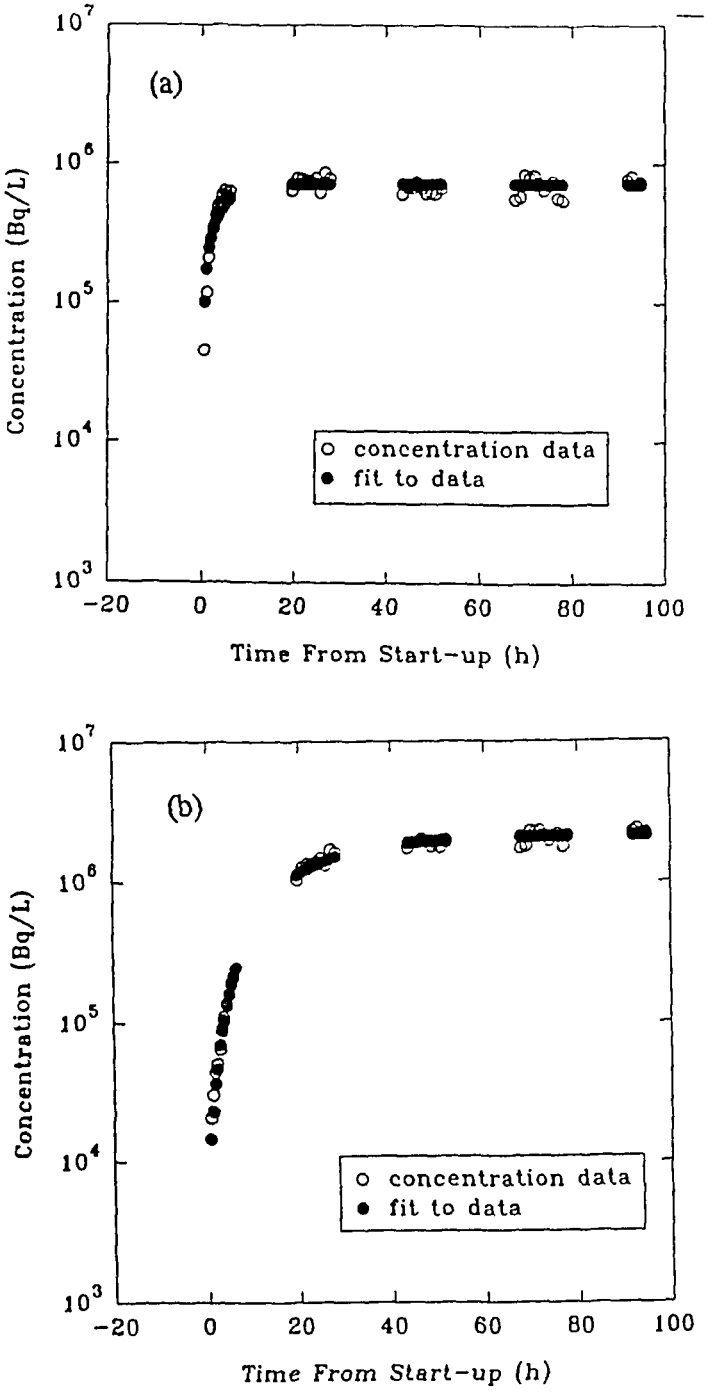

Figure 11: The concentration of (a) Kr-88 and (b) Xe-135 in the U of T reactor container water.

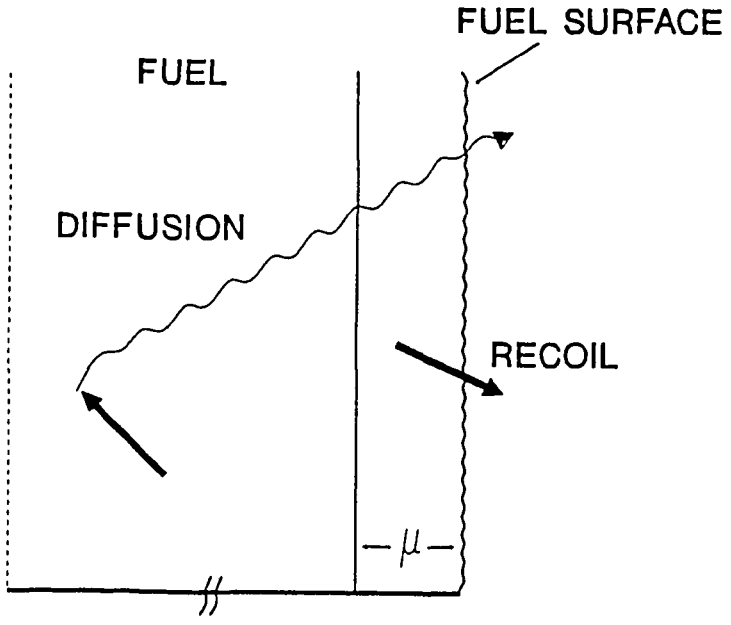

Figure 12: Schematic of diffusion and recoil release processes.

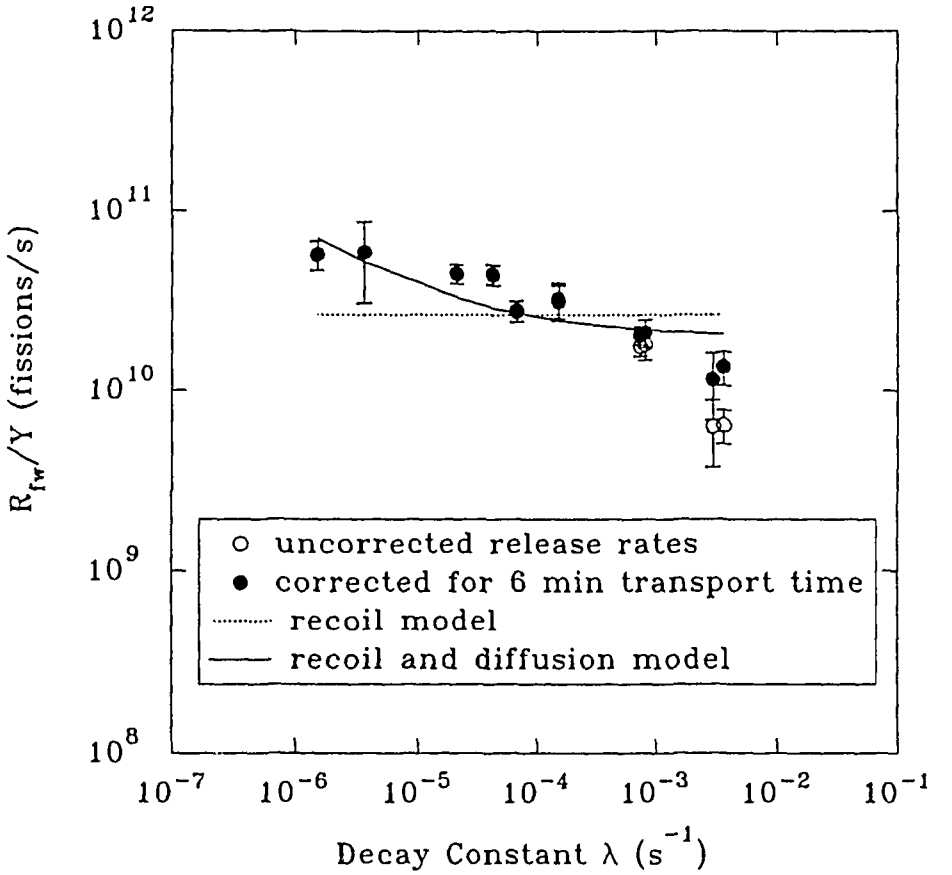

Figure 13(a): R_{fw}/Y versus λ plot for U of T reactor.
(The error bars indicate 95% confidence limits.)

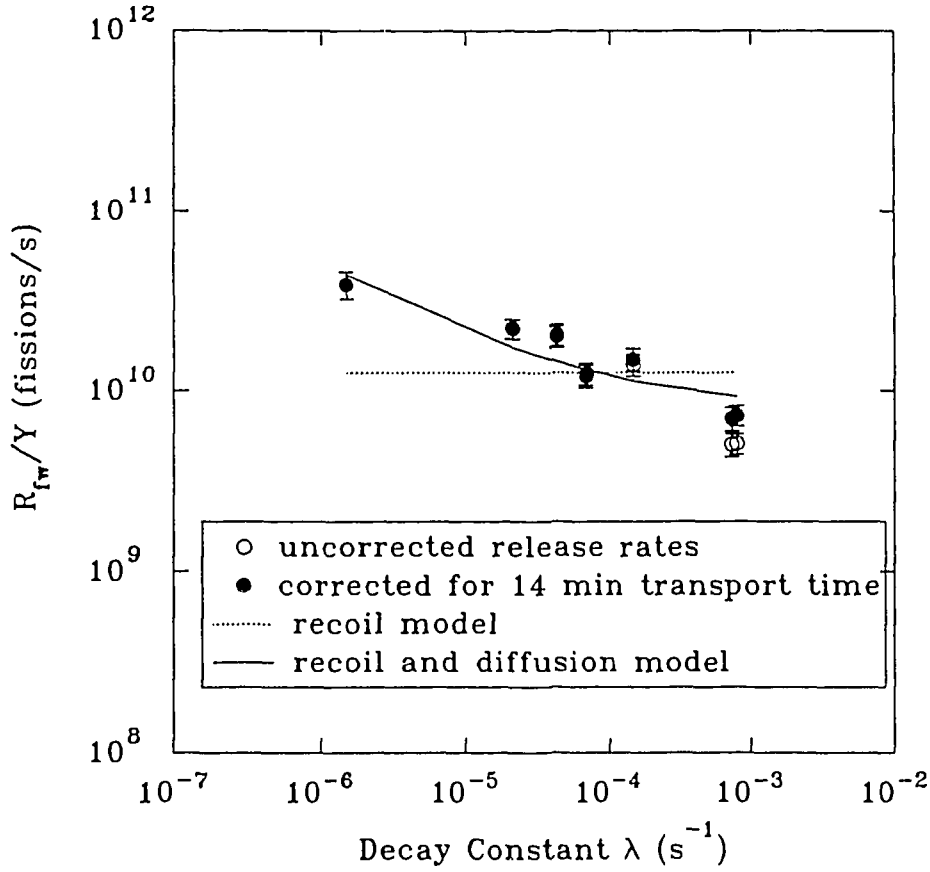

Figure 13(b): R_{fw}/Y versus λ plot for EP reactor.
(The error bars indicate 95% confidence limits.)

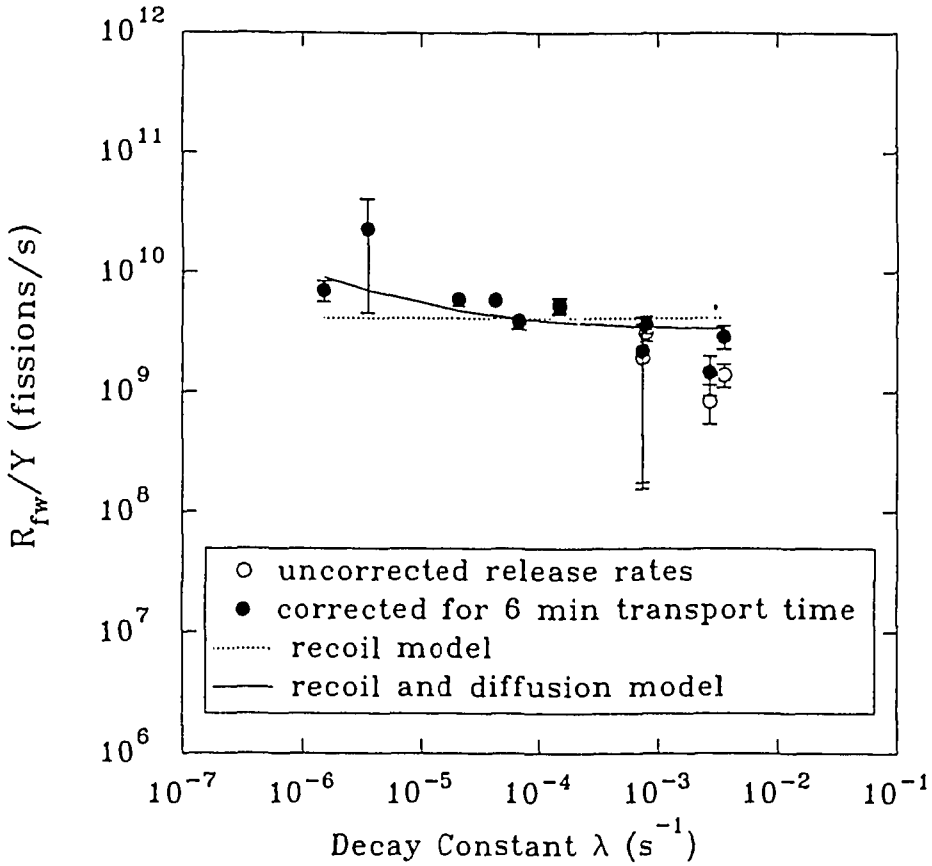

Figure 13(c): R_{fw}/Y versus λ plot for KIPF reactor.
(The error bars indicate 95% confidence limits.)

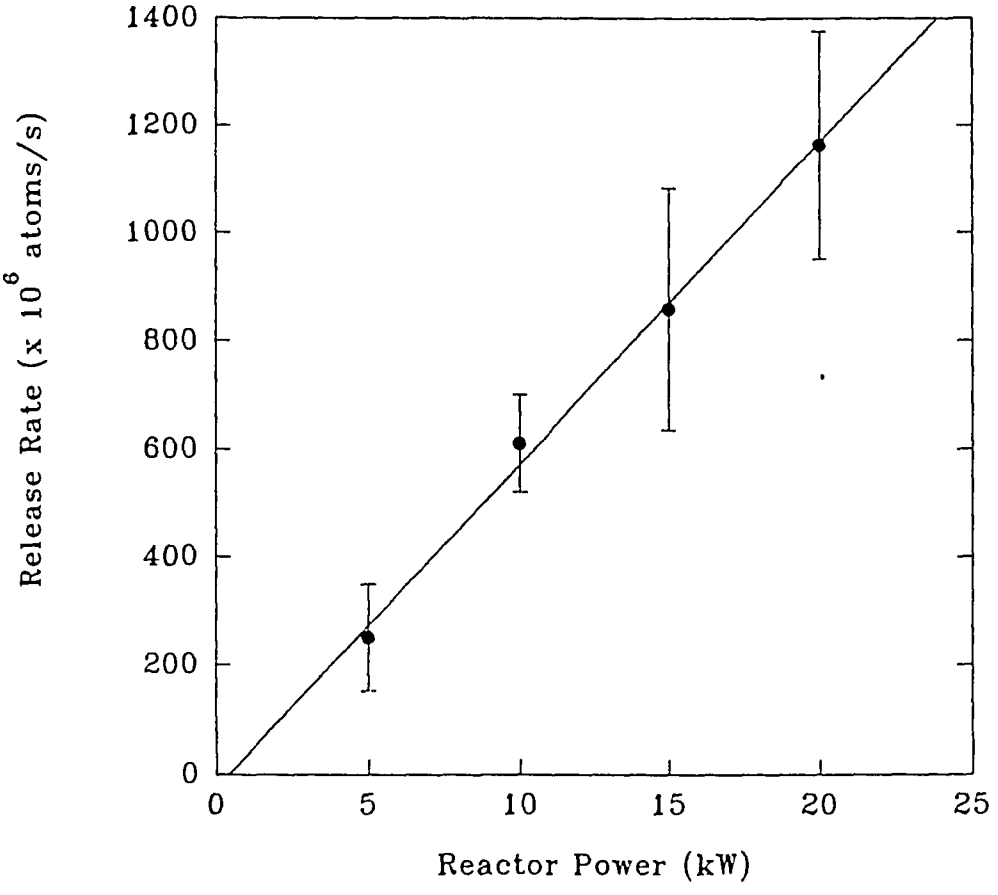

Figure 14: Release rate of ^{138}Xe (fuel-to-water) at KIPF reactor as a function of reactor power. (The error bars indicate 95% confidence limits.)

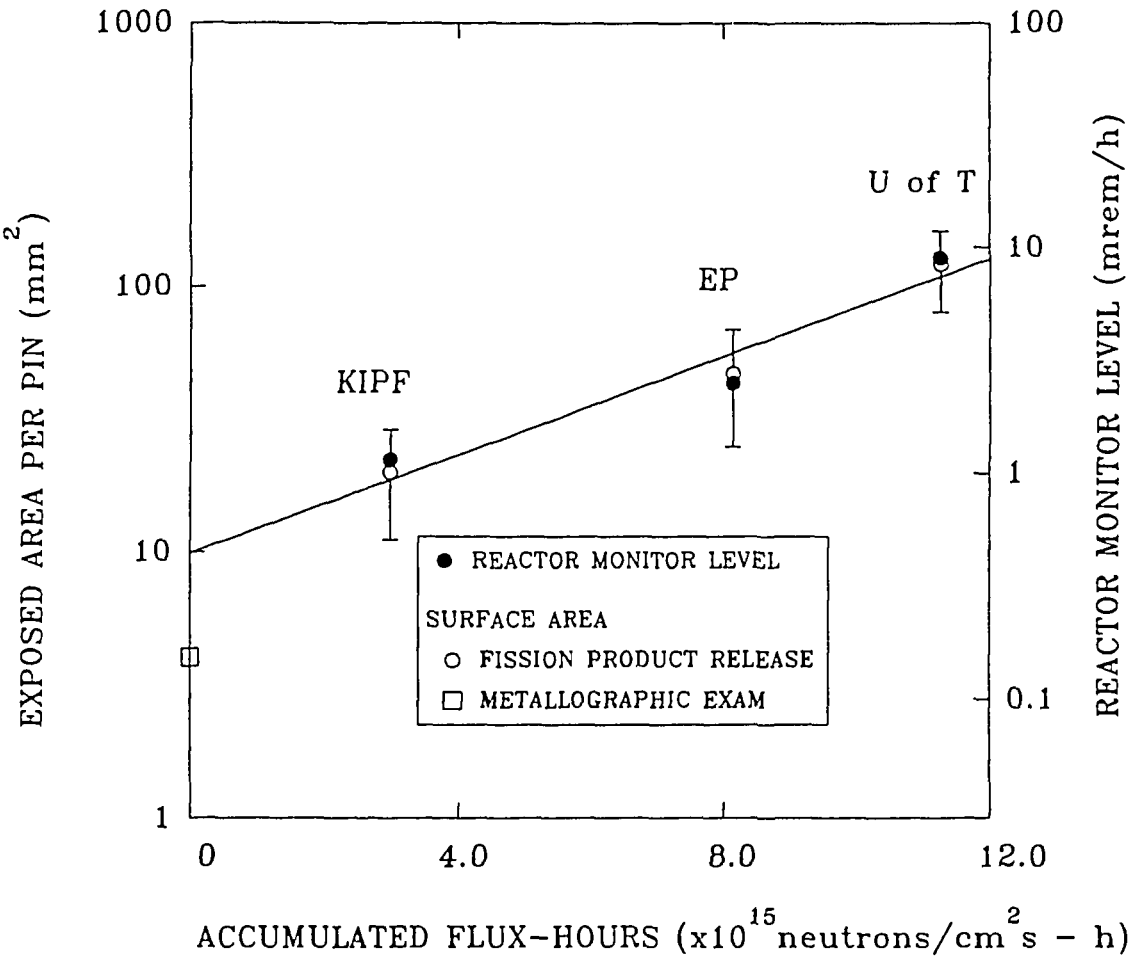

Figure 15: Increasing exposed fuel and alarm levels with burnup for U of T, EP and KIPF reactors. (The error bars indicate 95% confidence limits.)

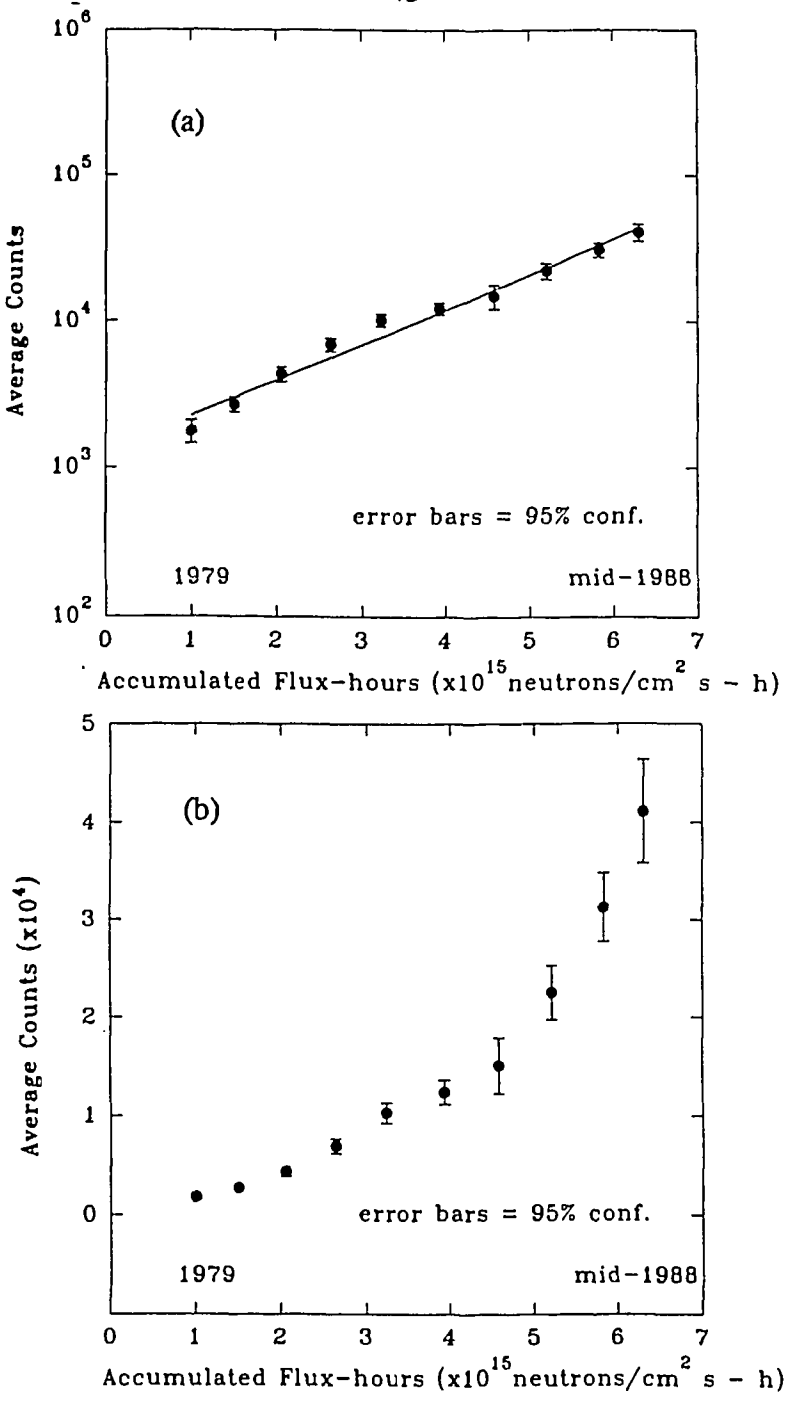

Figure 16: The weekly activity concentration of Xe-133 (averaged over a year) in the SLOWPOKE-2 reactor at Ecole Polytechnique versus the accumulated flux hours. (The concentration has been recorded as part of the routine maintenance at this facility.) Inspection of the semi-log plot (a) and the linear plot (b) indicate that the Xe-133 activity concentration varies as a non-linear phenomenon with burnup. (The error bars indicate 95% confidence limits.)

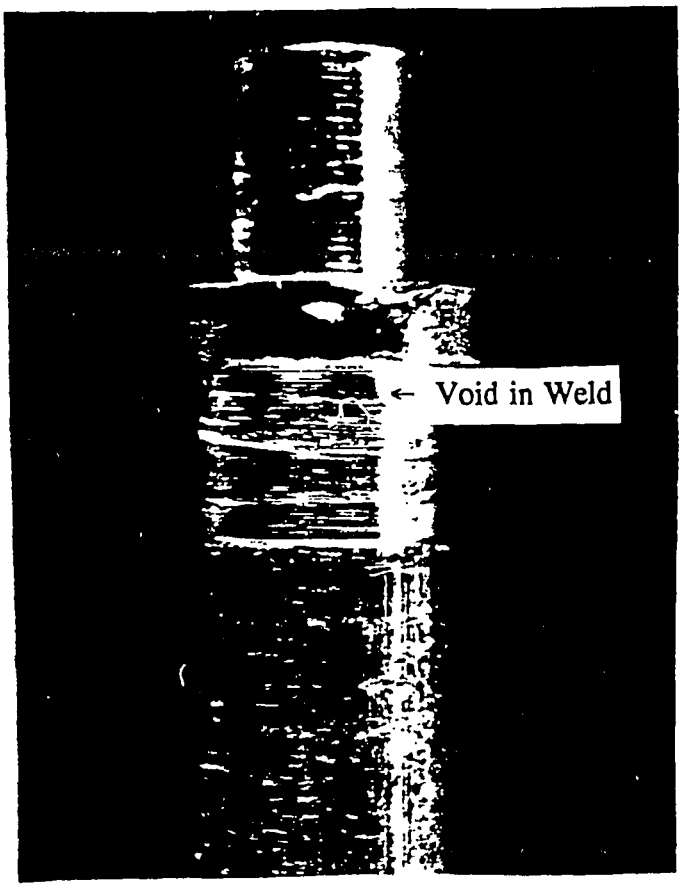

Figure 17(a): Visual inspection of an archive HEU SLOWPOKE-2 fuel pin showing voids in the machined weld zone. (Courtesy of Atomic Energy of Canada Limited.)

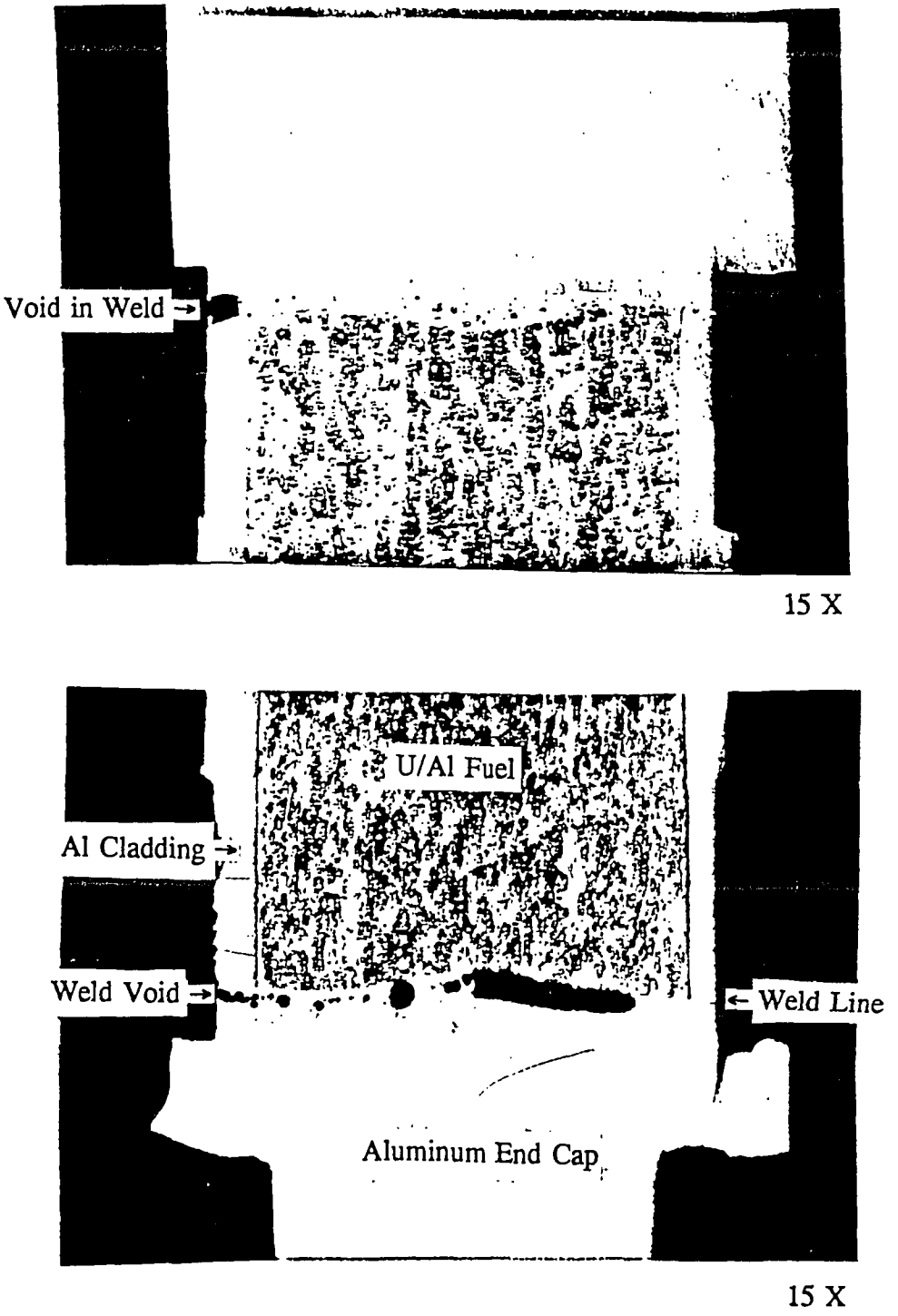

Figure 17(b): Metallographic examination of an archive HEU SLOWPOKE-2 fuel pin showing large voids in the end-weld line and sheath. A band of exposed fuel material can also be seen. (Courtesy of Atomic Energy of Canada Limited.)

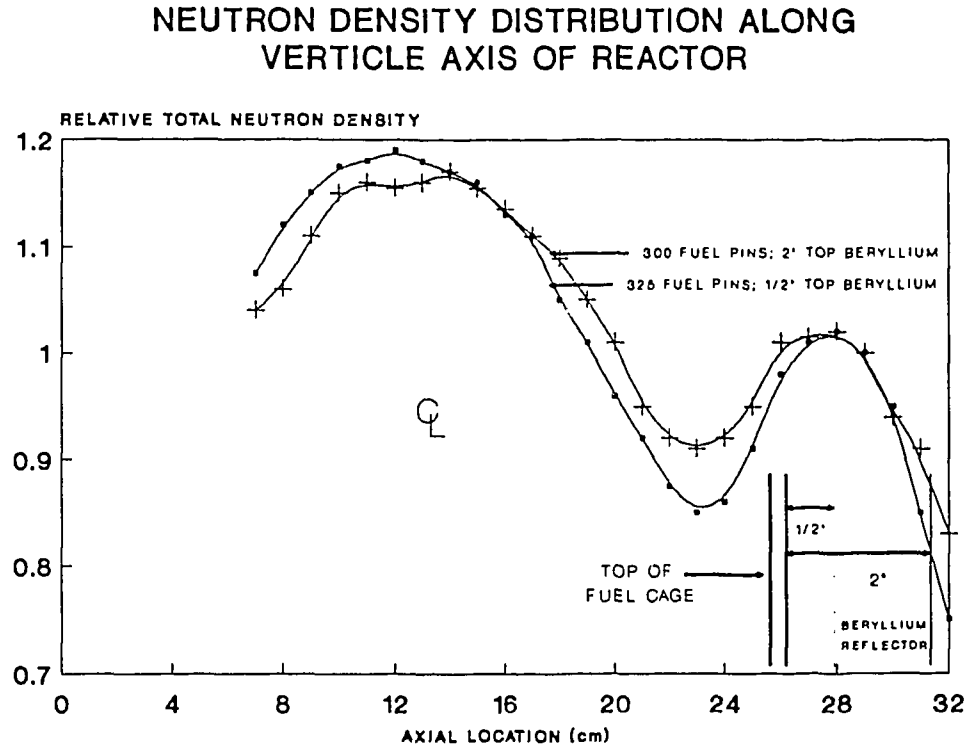

Figure 18 : Axial neutron flux distribution of a SLOWPOKE-2 reactor with 1/2" and 2" of beryllium added to the upper shim tray. (Taken from Reference 2.)

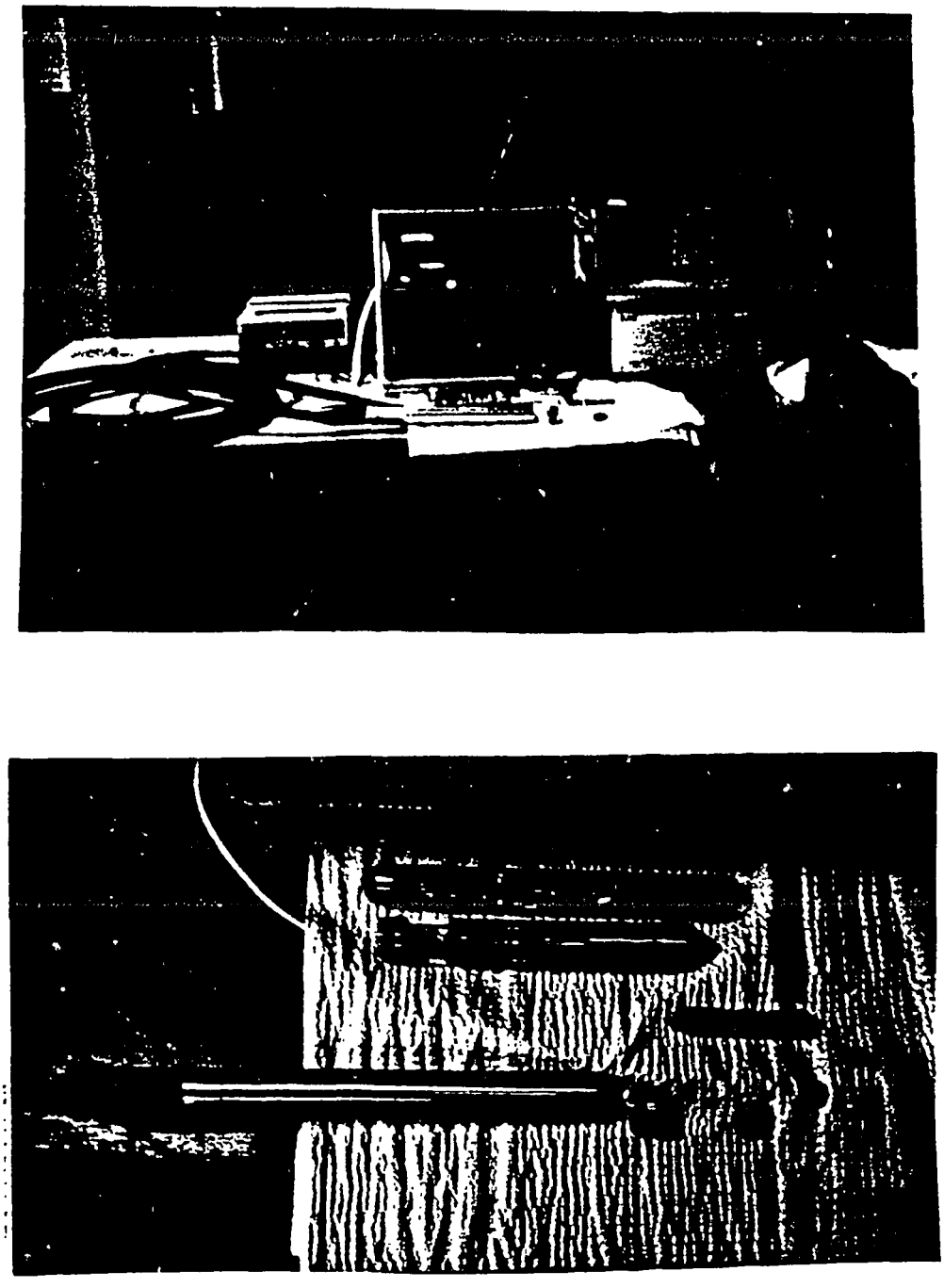

Figure 19: Underwater television camera used for the EP core visual examination.

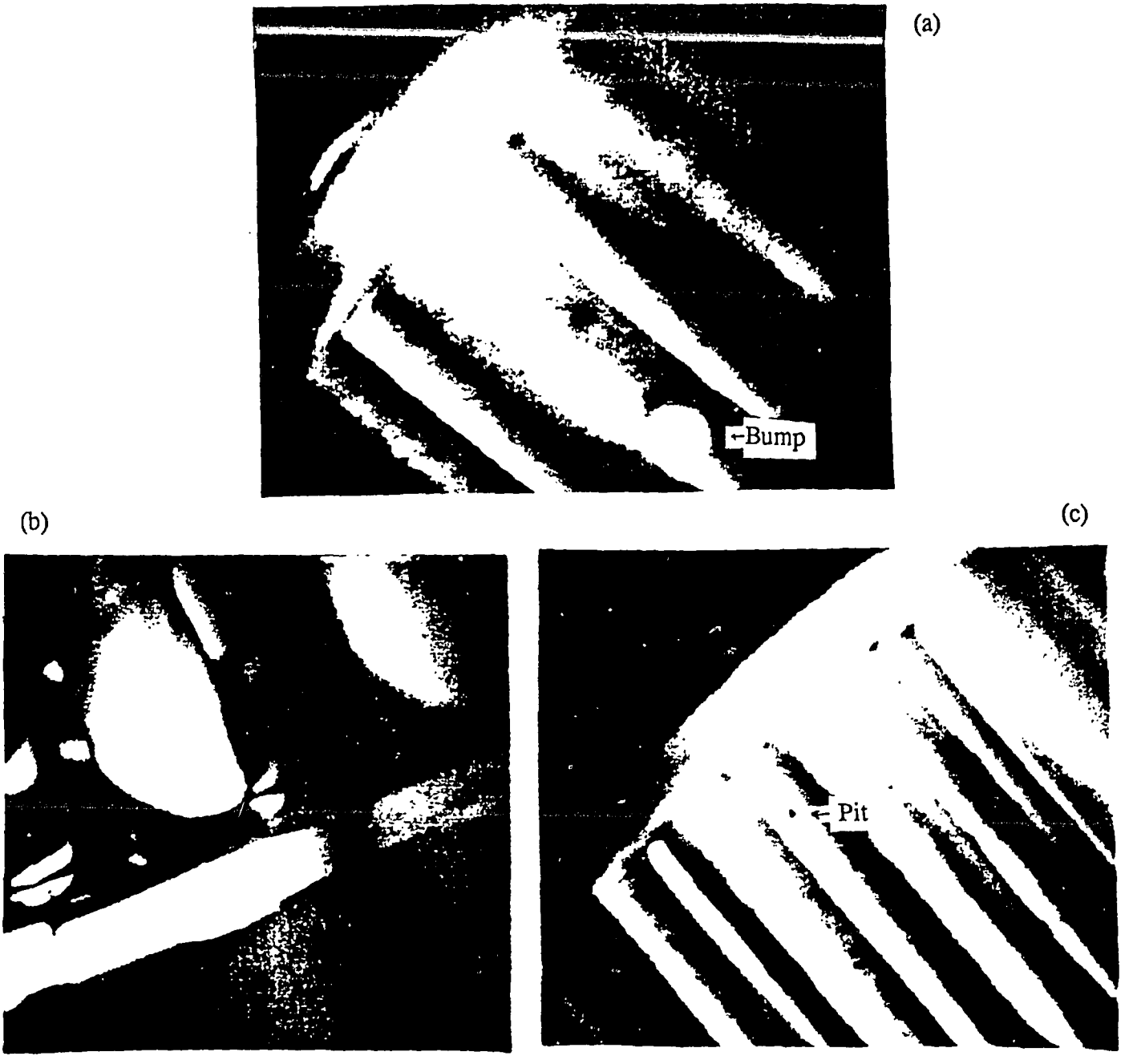

Figure 20: Results of the EP visual core examination with an underwater television camera.

(a) Small bump seen near the top of a fuel pin;
(b) Swelling at the bottom of a fuel pin;
(c) Visual of end-weld area at the top of the core showing no discernable evidence of deterioration. A small "pit" in the clad is also observed.

REFERENCES

1. A.D. Smith and B.M. Townes, "Description and Safety Analysis for the SLOWPOKE-2 Reactor with LEU Oxide Fuel", Atomic Energy of Canada Limited, Chalk River Laboratories, Report no. CPR-77, January 1985.

2. M.E. Wise and R.E. Kay, "Description and Safety Analysis for the SLOWPOKE-2 Reactor", Atomic Energy of Canada Limited, Radiochemical Company, Report no. CPR-26 (Rev.1), September 1983.

3. P.A. Beeley, L.G.I. Bennett, H.W. Bonin, L.S. Fisher and L.S. Wright, "The SLOWPOKE-2 Facility at the Royal Military College: Improved Performance and Versatility", Proceedings of the 8th Annual Conference of the Canadian Nuclear Society, Saint John, New Brunswick, 1987.

4. W.E. Downs, M.E. Wise and M.B. Anderson, "SLOWPOKE-2 Nuclear Reactor Description", Atomic Energy of Canada Limited, Commercial Products, Report no. CPSR-291, Rev. 4, April 1985.

5. "MicroSAMPO Advanced Gamma Spectrum Analysis Software - Version 2.0", User's Guide, Canberra Nuclear Products Group, CISE 511, September 1989.

6. L.A. Currie, "Limits for Qualitative Detection and Quantitative Determination", Anal. Chem. 40 (1968) 587.

7. B.J. Lewis, R.G.V. Hancock, D. Cole and L.G.I. Bennett, "A Preliminary Analysis of Fission Product Release in the HEU-Fueled SLOWPOKE-2 Reactor", Proceedings of the 11th Annual Conference of the Canadian Nuclear Society, Toronto, 1990, p. 6.29.

8. B.J. Lewis, "Fission Product Release from Nuclear Fuel by Recoil and Knockout", J. Nucl. Mater. 148 (1987) 28.

9. B.J. Lewis, "Fundamental Aspects of Defective Nuclear Fuel Behaviour and Fission Product Release", J. Nucl. Mater. 160 (1988) 201.

10. C.A. Wills, "User Guide for SUMRT", Atomic Energy of Canada Limited, Unpublished report, 1982.

11. A. Savitzky and M. Golay, "Smoothing and Differentiation of Data by Simplified Least Squares Procedure", Anal. Chem. 36 (1964) 1627.

12. "SigmaPlot Scientific Graphing Software", User's Manual, Version 4, Jandel Scientific, Corte Madera, California (1990).

13. S.L. Jurgilas, "Direct and Cumulative Fission Product Yields Based on ENDF/B-V", Atomic Energy of Canada Limited, Chalk River Laboratories, Report no. CRNL-2478, February 1983.

14. A.H. Booth, "A Suggested Method for Calculating the Diffusion of Radioactive Rare Gas Fission Products from UO_2 Fuel Elements and a Discussion of Proposed In-Reactor Experiments that May be Used to Test its Validity", Atomic Energy of Canada Limited, Report no. AECL-700, September 1957.

15. M.C. Billone, Y.Y. Liu, E.E. Gruber, T.H. Hughes and J.M. Kramer, "Status of Fuel Modeling Codes for Metallic Fuels", Proc. Int. Conf. Reliable Fuels for Liquid Metal Reactors, Tucson, Arizona, September 7-11, 1986.

16. J.M. Beeston, R.R. Hobbins, G.W. Gibson and W.C. Francis, "Development and Irradiation Performance of Uranium Aluminide Fuels in Test Reactors", Nucl. Technol. 49 (1980) 136.

17. J.A. Turnbull and C.A. Friskney, "The Diffusion Coefficients of Gaseous and Volatile Species During the Irradiation of Uranium Dioxide", J. Nucl. Mater. 107 (1982) 168.

18. H. Matzke, "Diffusion in Ceramic Oxide Systems", Advances in Ceramics, Vol. 17, American Ceramic Society (1986) p. 33.

19. D.R. Olander, "Fundamental Aspects of Nuclear Reactor Fuel Elements", US Department of Energy, TID-26711-p1, 1976, p. 303.

20. C. Wise, "Recoil Release of Fission Products from Nuclear Fuel", J. Nucl. Mater. 136 (1985) 30.

21. L.C. Northcliffe and Schilling, Nuclear Data Tables 7A (1970) 233.

22. G. Friedlander, J. Kennedy, E. Macias and J. Miller, "Nuclear and Radiochemistry", 3rd Edition, John Wiley and Sons, New York, 1981.

23. J.F. Ziegler, "TRIM-89 The Transport of Ions in Matter - Version 5.1", International Business Machines (IBM) - Radiation Science Group, User's Manual, November 1988.

24. G. Haverland, SLOWPOKE FACILITY, University of Alberta, Private Communication, May 1992.

25. G.G. Kennedy, Laboratoire Polyfonctionnel SLOWPOKE, Ecole Polytechnique, Private Communication, March 1992.

26. J.P. Murphy, P.J. Valliant, E.G. McVey and P.W. Reynolds, "Examination of SLOWPOKE-2 Reactor Fuel Elements at the Chalk River Laboratories", Atomic Energy of Canada Limited, Chalk River Laboratories, Report no. RC-827, March 1992 (draft).

27. C. Guertin, "Calcul du Coefficient de Temperature du Reacteur SLOWPOKE-2", Masters' Thesis, Institut de Genie Energetique, Ecole Polytechnique, Montreal, 1991.

28. W.Krull, "Standardization of Specifications and Inspection Procedures for LEU Plate-type Research Reactor Fuels", RERTR Programme Int. Meeting, Tennessy, 1986, p.159-172.

29. K. Vinjamuri and R.R. Hobbins, "Aqueous Corrosion of Uranium Aluminide Fuel", Nucl. Technol. 62 (1983) 145.

30. J.W. M^{c}Whirter and J.E. Draley, "Aqueous Corrosion of Uranium and its alloys: survey of project literature", Argonne National Laboratories, Report no. ANL-4862 (1952).

ACKNOWLEDGEMENTS

The authors would like to extend their sincere thanks to the many individuals who were involved in this project.

Thanks are especially due to the staff of the Atomic Energy Control Board (AECB) for their continued support and guidance of the project. We are much indebted to the following SLOWPOKE-2 operators who modified their busy work schedules, and extended their hospitality and assistance during the weeks of experimentation (including the lifting of one tonne of lead shielding!): R.G.V. Hancock (U of T), G.G. Kennedy (EP), and G.A. Burbidge, M. Mueller and A. Anderson (NORDION). The authors would also like to thank G.G. Kennedy for "volunteering" his reactor for the visual examination. Many thanks are due to J.P. Murphy (CRL), G.A. Burbidge and A. Anderson (NORDION) for their dedicated work on the visual examination. The authors would also like to acknowledge the help of R.D. MacDonald, P.J. Fehrenbach, and P.J. Valliant (CRL) for the metallographic study. Finally, the authors would like to thank J.W. Hilborn (CRL), J.R. Robertson (RNC), and B. Cox (U of T) for their helpful discussions, and D.R. Olander (University of California - Berkeley) for the TRIM code.

This work was funded by the Atomic Energy Control Board (research contract 2.197.1), the Academic Research Program of the Department of National Defence (allocation number 3705-902), and Atomic Energy of Canada Limited.

APPENDIX

RELEASE RATE FOR ISOTOPES WITH LONG-LIVED PRECURSORS

1. One Long-Lived Precursor

Most of the noble gas isotopes released into the reactor container water in Table 4 have relatively short-lived precursors. For a short-lived precursor, an equilibrium situation will be developed quickly. For nuclides with longer-lived precursors, the time dependence of this second source becomes important. The mass balance equations for the inventory (N) in the water of a given parent (1) and daughter (2) nuclide are:

$$dN_1/dt = R_1 - \lambda_1 N_1 \tag{1a}$$

$$dN_2/dt = R_2 + f\lambda_1 N_1 - \lambda_2 N_2, \tag{1b}$$

where f is the isotopic branching ratio, and R is a constant release rate. The solution to Equation (1a) is:

$$N_1(t) = N_{10} \exp(-\lambda_1 t) + (R_1/\lambda_1)(1 - \exp(-\lambda_1 t)) \quad . \tag{2}$$

Equation (2) can be inserted into Equation (1b) and solved yielding:

$$\begin{aligned} N_2(t) = {} & N_{20} \exp\{-\lambda_2 t\} + [(fR_1 + R_2)/\lambda_2]\cdot(1 - \exp\{-\lambda_2 t\}) \\ & + [f(\lambda_1 N_{10} - R_1)/(\lambda_2 - \lambda_1)]\cdot (\exp\{-\lambda_1 t\} - \exp\{-\lambda_2 t1\}) \end{aligned} \tag{3}$$

where the initial conditions $N_1(0)=N_{10}$ and $N_2(0)=N_{20}$ are known.

If the release into the water is due to recoil (see Section 5), the release rate R_1 will be proportional to the cumulative yield Y_1^c, which accounts for production due to the decay of the earlier chain members, whereas the release rate of the daughter product R_2 will depend on the direct fission yield, Y_2^d. Hence, using the relation

$$R_1/R_2 = Y_1^c/Y_2^d \quad , \tag{4}$$

and by defining

$$R_2^c = fR_1 + R_2 = R_2(1 + fY_1^c/Y_2^d) \quad , \tag{5}$$

Equation (3) becomes:

$$\begin{aligned} N_2(t) = {} & N_{20} \exp\{-\lambda_2 t\} + [R_2^c/\lambda_2]\cdot(1 - \exp\{-\lambda_2 t\}) \\ & + [f(\lambda_1 N_{10} - R_2^c Y_1^c/(Y_2^d + Y_1^c))/(\lambda_2 - \lambda_1)]\cdot(\exp\{-\lambda_1 t\} - \exp\{-\lambda_2 t\}) \end{aligned} \tag{6}$$

The release rate R_2^c which is the only unknown in Equation (6) was evaluated using a least-squares fit of Equation (6) to the concentration data (see Section 4.3).

2. Two Long-Lived Precursors

A similar analysis is required for the isotopes ^{133}Xe and ^{135}Xe, except that three mass balance equations must be solved in order to account for the production of the isotope from both the parent (^{133}I and ^{135}I), and its isomer (^{133m}Xe and ^{135m}Xe). The three mass balance equations for this situation are:

$$dN_1/dt = R_1 - \lambda_1 N_1 \tag{7a}$$

$$dN_2/dt = R_2 + f\lambda_1 N_1 - \lambda_2 N_2, \tag{7b}$$

$$dN_3/dt = R_3 + (1-f)\lambda_1 N_1 + \lambda_2 N_2 - \lambda_3 N_3 \tag{7c}$$

where the parent decays to the isomeric state of the daughter (2) with a branching fraction f, and to the ground state of the daughter (3) with a fraction (1-f). The meta-stable state of the daughter (2) decays directly to its ground state (3).

Using the solutions of Equations (2) and (3), Equation (7c) can be solved as

$$\begin{aligned} N_3(t) = {} & N_{30}\exp\{-\lambda_3 t\} + [(R_1 + R_2 + R_3)/\lambda_3]\cdot(1 - \exp\{-\lambda_3 t\}) \\ & + [N_{20} - (fR_1+R_2)/\lambda_2 - f(\lambda_1 N_{10} - R_1)/(\lambda_2 - \lambda_1)]\cdot[\lambda_2/(\lambda_3 - \lambda_2)] \text{ x} \\ & \quad \text{x } (\exp\{-\lambda_2 t\} - \exp\{-\lambda_3 t\}) \\ & + [(1-f)(N_{10} - R_1)/\lambda_1 + f\lambda_2(N_{10} - R_1/\lambda_1)/(\lambda_2 - \lambda_1)]\cdot[\lambda_1/(\lambda_3 - \lambda_1)] \text{ x} \\ & \quad \text{x } (\exp\{-\lambda_1 t\} - \exp\{-\lambda_3 t\}) \end{aligned} \tag{8}$$

where once again the initial conditions $N_1(0)=N_{10}$, $N_2(0)=N_{20}$, and $N_3(0)=N_{30}$ are known.

Employing the relations

$$R_1/R_2 = Y_1^c/Y_2^d \quad \text{and} \quad R_1/R_3 = Y_1^c/Y_3^d \ , \tag{9}$$

and defining R_3^c by

$$R_3^c = R_1 + R_2 + R_3 \ , \tag{10}$$

Equation (8) becomes:

$$N_3(t) = N_{30}\exp\{-\lambda_3 t\} + [R_3^c/\lambda_3]\cdot(1 - \exp\{-\lambda_3 t\})$$
$$+ [N_{20} - R_3^c(Y_2^d + fY_1^c)/Y_3^c\lambda_2 - f(\lambda_1 N_{10} - R_3^c Y_1^c/Y_3^c)/(\lambda_2 - \lambda_1)]\cdot[\lambda_2/(\lambda_3 - \lambda_2)] \times$$
$$\times (\exp\{-\lambda_2 t\} - \exp\{-\lambda_3 t\})$$
$$+ [(1-f)(N_{10} - R_3^c Y_1^c/Y_3^c\lambda_1) + f\lambda_2(N_{10} - R_3^c Y_1^c/Y_3^c\lambda_1)/(\lambda_2 - \lambda_1)]\cdot[\lambda_1/(\lambda_3 - \lambda_1)] \times$$
$$\times (\exp\{-\lambda_1 t\} - \exp\{-\lambda_3 t\}) \qquad (11)$$

Here $Y_3^c = Y_1^c + Y_2^d + Y_3^d$ is defined as the cumulative yield of the daughter isotope. The release rate R_3^c was evaluated using a least-squares fit of Equation (11) to the concentration data for Xe-135 and Xe-133.